Chapter 8
Mercury in Aquatic Systems of North Patagonia (Argentina): Sources, Processes, and Trophic Transfer

María del Carmen Diéguez, Marina Arcagni, Andrea Rizzo, Soledad Pérez Catán, Carolina Soto Cárdenas, Milena Horvat, and Sergio Ribeiro Guevara

1 Overview of Mercury in the Environment

Mercury (Hg) is a global pollutant of serious concern due to its toxicity, persistence, and mobility in the environment. Currently, regions of the world that are remote and devoid of natural and/or anthropogenic sources of Hg show the impact of this toxic metal due to its long-range atmospheric transport and deposition (Driscoll et al. 2013; Obrist et al. 2018). As a consequence of the global presence of Hg, different Hg compounds have become ubiquitous in the environment and in food (Fernándes et al. 2020). The organic species monomethyl- and dimethylmercury (CH_3Hg and $(CH_3)_2Hg$, respectively) are potent neurotoxins that affect primarily the central nervous system. Elemental Hg (Hg^0) and inorganic mercury species (i.e., Hg salts) are also dangerous for human health, and their absorption through inhalation, contact, and ingestion can damage the gastrointestinal tract, the lungs and kidneys, the skin,

M. d. C. Diéguez (✉) · C. Soto Cárdenas
National Research Institute on Biodiversity and Environment (INIBIOMA), National Council of Technology and Science (CONICET), Comahue National University (UNComa), Aquatic Ecology at Landscape Scale Group, San Carlos de Bariloche, Argentina

M. Arcagni · S. Pérez Catán · S. Ribeiro Guevara
National Commission of Atomic Energy (CNEA), Neutronic Activation Analysis Laboratory, Nuclear Engineering Management, San Carlos de Bariloche, Argentina

A. Rizzo
National Commission of Atomic Energy (CNEA), Neutronic Activation Analysis Laboratory, Nuclear Engineering Management, San Carlos de Bariloche, Argentina

National Council of Technology and Science (CONICET, CCT Patagonia Norte), San Carlos de Bariloche, Argentina

M. Horvat
Jožef Stefan Institute, Department of Environmental Sciences, Ljubljana, Slovenia

G. Mataloni, R. D. Quintana (eds.), *Freshwaters and Wetlands of Patagonia*, Natural and Social Sciences of Patagonia,
https://doi.org/10.1007/978-3-031-10027-7_8

as well as the nervous and immune systems (Lehnherr 2014; WHO 2017). Due to its lipophilic nature, CH_3Hg bioaccumulates and biomagnifies in aquatic food webs more readily than other Hg species. Methylmercury causes long-term consequences at the ecosystem level and affects wildlife and human populations with fish-based diets (Driscoll et al. 2013; Eagles-Smith et al. 2016; Evers 2018; Whitney and Cristol 2018; Chételat et al. 2020). Several factors are determinant of the effects of Hg on wildlife and humans, including the type of Hg, the dose, the route and duration of exposure, and the developmental stage. The presence of CH_3Hg in wildlife is the result of the combination of ecological processes influencing dietary exposure and physiological processes regulating assimilation, transformation, and elimination (Ackermann et al. 2016; Chételat et al. 2020).

Mercury has a complex biogeochemical cycle involving its circulation among the lithosphere, the atmosphere, and the hydrosphere (Driscoll et al. 2013; Obrist et al. 2018). This element is naturally mobilized from lithospheric reservoirs to the atmosphere through volcanic and geological activity, rock weathering, and also volatilizes from surface waters, soils, and vegetation (Selin 2009; Driscoll et al. 2013). Humans have mobilized Hg from reservoirs to the atmosphere through mining, coal combustion, and industrial processes, altering its biogeochemical cycling by increasing drastically the atmospheric concentrations (~450%) and further deposition in ecosystems (Pirrone et al. 2010; Driscoll et al. 2013; UNEP 2018). Recent estimates indicate that anthropogenic Hg emissions (~2000 Mg yr^{-1}) exceed by far natural emissions (76–300 Mg yr^{-1}) (Streets et al. 2017, 2019). In addition to emissions, anthropogenic sources of Hg include direct releases to the aquatic environment, particularly from point sources, and the remobilization of historical deposition of Hg, and from legacy Hg deposits in contaminated sites (AMAP/UNEP 2013; Kocman et al. 2013). Archives of Hg deposition such as peat and lake sediments from remote regions indicate up to fivefold enrichment of Hg due to atmospheric deposition from the beginning of the industrial era (Streets et al. 2017; Gustin et al. 2020).

The behaviors of the different chemical forms of Hg play critical roles in its biogeochemical cycling. Gaseous elemental Hg (Hg^0), the predominantly emitted species and the one with the highest concentration in the atmosphere, has high chemical inertness facilitating its long-range transport before deposition (Sprovieri et al. 2010; Driscoll et al. 2013; Obrist et al. 2018; Lyman et al. 2020). Reactive gaseous Hg (mostly gaseous chloride and oxide forms of ionic Hg) and particle-bound Hg are more soluble in water and reactive than Hg^0, having a shorter residence time in the atmosphere (0.5 to 2 days and 0.5 to 3 days, respectively), depositing in local and regional ecosystems (Driscoll et al. 2007, 2013; Sprovieri et al. 2016; Obrist et al. 2018). Although there is uncertainty regarding the atmospheric redox chemistry of Hg, the halogen atoms are potentially important Hg^0 oxidants in the atmosphere with binding energies of the Hg compounds produced in the order HgCl > HgBr > HgI (Selin 2009; Driscoll et al. 2013). Therefore, depending on the speciation of the emissions and on the residence time in the atmosphere, Hg deposition may impact locally, regionally, or globally (Dastoor and Larocque 2004; Driscoll et al. 2007, 2013). Wet deposition consists mostly of reactive Hg^{2+}, gaseous

oxidized Hg (GOM), and particulate-bound Hg (PBM), scavenged by water droplets in the air, whereas Hg^0 is a major component of the total Hg in dry deposition along with Hg^{2+} in gaseous or particulate phase. Dry deposition of Hg^0 via plant uptake (stomatal gas exchange) is dominant in terrestrial vegetated ecosystems (Gustin et al. 2020). Thus, in forested ecosystems, litterfall is considered a major component of atmospheric deposition and its decomposition results in large inputs of Hg and organic matter (OM) to the soil (Grigal 2002). Also, gaseous and particulate Hg^{2+} depositing directly to the canopy are washed off by throughfall contributing to soil deposits (Graydon et al. 2008; Bishop et al. 2020). Conversion of deposited Hg^{2+} to the organic species monomethyl (CH_3Hg) and, to a limited extent, to dimethylmercury ($(CH_3)_2Hg$) occurs through biotic and abiotic processes in anoxic and/or oxygen-deficient sites of soils, wetlands, and aquatic systems. Sulfur, iron, and OM affect Hg^{2+} chemical speciation (Ravichandran 2004; Bravo and Cosio 2019).

Lakes receive atmospheric Hg inputs (mostly Hg^{2+}) directly through the surface, and, due to their lower position in the landscape, concentrate the Hg deposited in their catchments which is mobilized by runoff (Fig. 8.1). In particular, remote lakes at high elevation are currently subject to remarkable biochemical changes due to deposition of different elements, including C, N, S, and Hg, among others (Driscoll et al. 2007, 2013; Mladenov et al. 2011, 2012). The relative importance of atmospheric and watershed Hg sources varies depending on land use, hydrology, and the content and composition of dissolved organic matter (DOM) (Hsu-Kim et al. 2018; Obrist et al. 2018; Braunfireun et al. 2020). The C pool of the catchment plays a crucial role in the transport and cycling of Hg from terrestrial and aquatic systems.

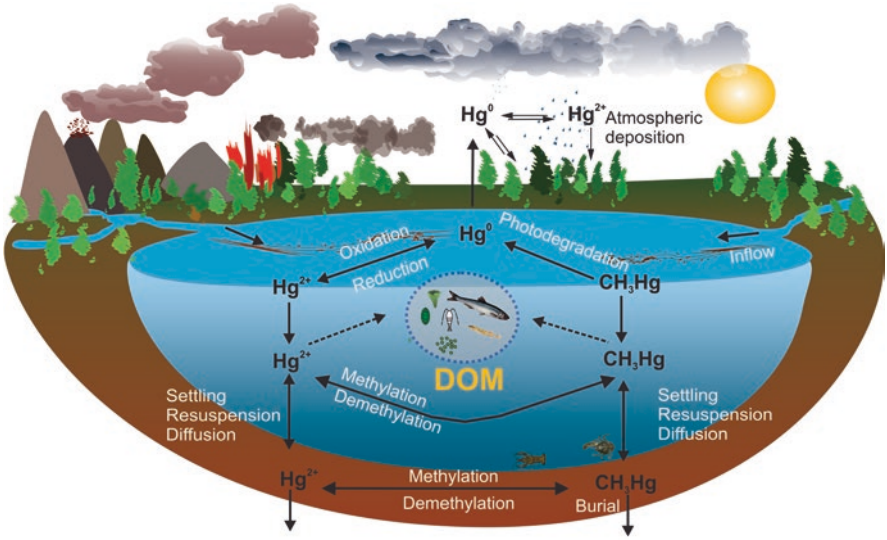

Fig. 8.1 Mercury cycling in catchments. References: Hg^0, elemental mercury; Hg^{2+}, ionic mercury; CH_3Hg, methylmercury; DOM, dissolved organic matter

Natural OM contains different amounts of thiols, which sulfhydryl group has a high capacity to complex Hg^{2+} and CH_3Hg. The concentration and molecular composition of the DOM pool determine Hg fractionation, availability, and biotic uptake, as well as the net Hg^{2+} methylation in aquatic systems (Ravichandran 2004; Bravo and Cosio 2019; Lavoie et al. 2019; Branfireun et al. 2020). In these ecosystems, Hg^{2+} can be either (i) reduced to Hg^0 and reemitted to the atmosphere, (ii) methylated to the organic form CH_3Hg, or (iii) bound to OM and inorganic particles, depositing on bottom sediments. CH_3Hg formed in aquatic ecosystems can also deposit on the sediments, be methylated, and/or form volatile $(CH_3)_2Hg$, although the latter pathway is still a matter of debate (Fig. 8.1) (Paranjape and Hall 2017; Zhu et al. 2018; Braunfireun et al. 2020). Part of $(CH_3)_2Hg$ can be reemitted to the atmosphere or degraded to CH_3Hg, which can also be biotically and/or abiotically demethylated (Marvin DiPasquale et al. 2000; Barkay et al. 2003; Schaefer et al. 2004; Fernández-Gómez et al. 2013). Most of the CH_3Hg present in headwaters is formed in situ or in the surrounding catchment and is subsequently transported into rivers, lakes, and oceans, concentrating in aquatic food chains (Chételat et al. 2020 and references therein).

2 Freshwaters in the Patagonian Landscape

Patagonia is a vast territory characterized by wide environmental gradients that reflect in the different landscapes from the Pacific to the Atlantic coast, from northern to southern locations, and from lowlands to high altitudes in the Andes. The headwaters of the region comprise complex fluvial networks of glacial origin born in the Andes, including mountain streams and lakes, deep and shallow piedmont lakes draining through large rivers toward the Atlantic and Pacific oceans (Chap. 9). In Andean North Patagonia (Argentina), aquatic systems occur along a bioclimatic gradient characterized by a west-to-east sharp decrease in the precipitation caused by the rain shadow effect of the Andes on the westerlies, which generates a transition from temperate forests near the Andes to a semidesert in less than 100 km to the east (Fig. 8.2a,b).

The Andean sector of Patagonia is located within the Southern Volcanic Zone, under the influence of active volcanoes (Andean volcanic belt) with several eruptions during the Holocene (Singer et al. 2008; Stern 2008). The Andean volcanic belt extends from 33° S to 46° S, and the emissions of gaseous elements and

Fig. 8.2 (continued) DH, Dina Huapi; PC, Puerto Cisne; BRC, San Carlos de Bariloche City; PCCVC, Puyehue Cordón Caulle Volcanic Complex. Red triangles indicate volcanoes. Numbers indicate sites in NHNP in which point measurements of atmospheric mercury have been performed (Horvat and Kotnik 2007). Sites 1, 2, 5, and 7 to 10: ~1 to ~3 ng m^{-3}; Point 3: ~15 ng m^{-3}; Point 4: ~15 and ~18 ng m^{-3}; Point 6: ~10 ng m^{-3}

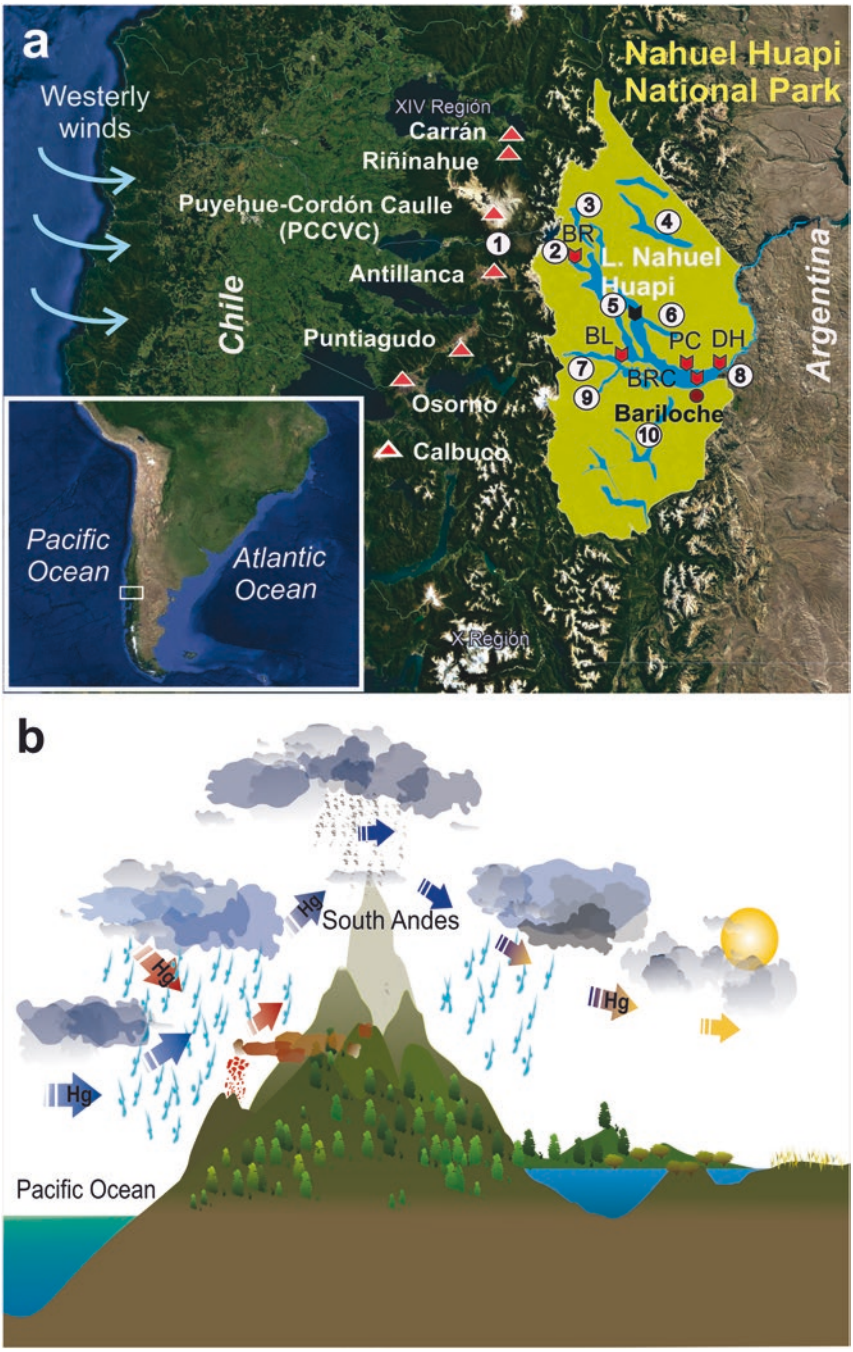

Fig. 8.2 (**a**) Map of Nahuel Huapi National Park, Patagonia, Argentina (green area) (Aerial Image from Google Earth). (**b**) Longitudinal section of the bioclimatic gradient within Nahuel Huapi National Park (North Patagonia, Argentina). References: BR, Brazo Rincón; BL, Bahía López;

pyroclastic material from active volcanoes impact the surrounding landscape, particularly at the eastern side of the Andes due to the action of the westerlies that promote transport and deposition. Consequently, in Andean Patagonian catchments, soils and lake sediment profiles show the historical accumulation of volcanic ash resulting from the intense volcanic activity of the Patagonian Andes (Ribeiro et al. 2005, 2010; Daga et al. 2008; Pereyra and Bouza 2019). Volcanic eruptions and forest fires are frequent disturbances in Andean Patagonia, shaping the structure and function of terrestrial and aquatic ecosystems and ultimately reflecting in biogeochemical cycling (Veblen and Kitzberger 2002; Diaz et al. 2013; Modenutti et al. 2013, 2016; Berenstecher et al. 2017; Holz et al. 2017; Beigt et al. 2019; Du Preez et al. 2020; see also Chaps. 3 and 7).

In North Patagonia, headwater catchments are included in protected areas since they are unique biomes and reservoirs of biodiversity. The Nahuel Huapi National Park (NHNP, 40° 08'–41° 35' S; 71° 01'–71 57' W; 7,173 km^2 surface) is the largest natural reserve of North Patagonia and comprises the Nahuel Huapi lake catchment, which includes the headwaters of the major fluvial network of North Patagonia (Fig. 8.2a). The topography of NHNP is characterized by Andean mountains and valleys at the western stretch, grading in altitude toward formations of sierra and meseta at the east (Fig. 8.2b). Glacial and volcanic processes shape the landscape. The climate is cold temperate and precipitation ranges from ~3500 mm yr^{-1} at the west to ~500 mm yr^{-1} at the east of the park. The precipitation pattern is highly seasonal with ~60% of the annual precipitation, concentrated between May and September (austral autumn and winter). Along this environmental gradient, three bioclimatic units can be distinguished from west to east: the High Andean district above the tree line, forested areas including hyperhumid, humid, and subhumid forests of *Nothofagus* spp., and the steppe (Fig. 8.2b) (Ferreyra et al. 1998; Mermoz et al. 2009; Queimaliños et al. 2019).

Topography, vegetation, climate characteristics (i.e., seasonality and precipitation), and lake morphometry are chief drivers of airshed-watershed interactions, determining the circulation patterns of materials within the landscape. Linkages between terrestrial and aquatic environmental matrices depend on ecosystems properties and climate, and, thereby, they are influenced by regional and global trends. In NHNP, the marked bioclimatic gradient reflects in the biogeochemical patterns of lakes. In fact, climate-vegetation co-effects have been shown to drive the timing, quantity, and quality of the terrestrial inputs to deep and shallow lakes and running waters, as revealed through changes in their DOM pools (Queimaliños et al. 2012, 2019; García et al. 2015a, b; Soto Cárdenas et al. 2017; Zagarese et al. 2017). DOM is a main transporter of terrestrial C, nutrients, and Hg toward aquatic systems. In NHNP, lakes at the western end of the gradient display comparatively higher terrestrial signatures (particularly during the wet season), due to the enhanced hydrological connectivity and the contribution of native forests. Despite differences in the amount and quality of terrestrial inputs, deep Andean lakes show similar properties in nutrient and dissolved organic carbon (DOC) concentrations corresponding to oligo- and ultraoligotrophic conditions, whereas shallow lakes are a more heterogeneous group, encompassing ultraoligo- to mesotrophic systems (Díaz et al. 2007;

Queimaliños et al. 2012, 2019; Soto Cárdenas et al. 2017, 2018a). Deep lakes are warm monomictic, showing thermal stratification in late spring and summer, and developing the thermocline between 30 and 40 m (Queimaliños et al. 1999; Pérez et al. 2002). In contrast, shallow lakes are usually polymictic, freezing occasionally in harsh winters and showing thermal stratification in late spring or early summer (Soto Cárdenas et al. 2017).

The waters have low specific conductivity (<50 μS cm^{-1}) and circumneutral pH. Low DOC (~0.25–4 mg L^{-1}) and chlorophyll *a* (~0.1–1.5 μg L^{-1}) concentrations determine optically thin water columns, resulting in high underwater irradiance and extended euphotic zones (ca. 40 m) in deep lakes, and in water columns illuminated up to the bottom in the case of shallow lakes (Morris et al. 1995; Queimaliños et al. 2012, 2019; Soto Cárdenas et al. 2017). Chlorophyll *a* concentration shows remarkable variation in the vertical profile, especially in deep lakes, which characterize by the occurrence of metalimnetic peaks in summer due to the patchy vertical distribution of algae-bearing mixotrophic ciliates and flagellates (Queimaliños et al. 1999, 2002, 2012, 2019; see also Chap. 3).

3 Mercury in Andean Patagonian Catchments

Understanding the fate of Hg in aquatic systems requires a comprehensive approach due to the nature and ubiquity of this pollutant and to the fact that aquatic systems concentrate materials from their catchments, reflecting atmospheric as well as terrestrial processes. For two decades and in the light of the pieces of evidence gathered, the focus of Hg research in Andean Patagonian environments moved progressively toward a catchment perspective. Ecosystems of the region still have many areas to be explored and processes to be unveiled. Studies of Patagonian ecosystems usually face the need to step back from a goal to resolve fragmentary environmental information essential to move forward. The following sections aim at providing the reader with critical elements to understand the occurrence and cycling pathways of Hg in a large and pristine headwater catchment of North Patagonia, involving studies on different environmental compartments of NHNP (Fig. 8.2a).

3.1 First Records of Mercury in Andean Patagonian Catchments: Evidence from the Analysis of Lake Sediment Sequences (Legacy Mercury/Historical Mercury)

Most Hg research in the Argentinean Patagonia has been carried out in pristine headwaters including high-altitude lakes (mountain lakes) and deep and shallow piedmont lakes of Northwestern Patagonia. The most extensive body of work has been gathered in NHNP. Early research focusing on the occurrence of metals in

Lake Nahuel Huapi (764 m a.s.l; 557 km^2 surface; 464 m maximum depth) detected the presence of Hg above background levels in sedimentary sequences and in the suspended load in the water column at different lake sites (Ribeiro Guevara et al. 2002). Later, a screening of shallow and deep lakes belonging to the Nahuel Huapi catchment (Nahuel Huapi, Moreno West, Morenito, Espejo Chico, and Escondido) and Lake Traful evaluated Hg concentrations in sediment profiles, revealing two background Hg levels. Lower total Hg (THg) levels, ranging from ~0.08 to 0.21 μg g^{-1}, were associated with preindustrial times, while higher levels, ~0.17 to 0.32 μg g^{-1}, were associated with modern times (Ribeiro Guevara et al. 2005). In the upper layers of sediment cores from most of the studied lakes, dated to the second half of the twentieth century, the THg concentrations were even higher (from 0.5 to 3 μg g^{-1}) indicating moderate Hg contamination. In deeper layers, Hg concentrations three- to fivefold above background levels were observed, suggesting natural Hg inputs during the past millennium. Other studies based on sediment cores from the mountain lake Tonček and the piedmont lake Moreno West also detected high preindustrial Hg levels. In the Hg concentration profiles of both lakes, two sections were identified in the core with values up to tenfold the background level (0.05 μg g^{-1}), corresponding to the thirteenth century, and to the eighteenth and nineteenth centuries, with values compatible with contamination (0.40 to 0.65 μg g^{-1}), suggesting the impact of regional events (Ribeiro Guevara et al. 2010). Increased Hg concentrations were detected immediately above some tephra layers, pointing to a link with volcanic events. Besides, deep Hg peaks were found coinciding with charcoal peaks, both matching with evidence arising from tree-ring data and historical records of extended forest fires (Ribeiro Guevara et al. 2010). Thus, in the studied catchment (Fig. 8.2a), lake sediment archives reflect the frequent disturbances caused by volcanic eruptions and forest fires and the departure of Hg concentrations from background levels attributable to the global cycling of Hg in modern times.

At a wider regional scale, the analysis of sediment sequences from other lakes in southern Patagonia supported the connection between increased THg levels in the sediments, volcanic events, and widespread fires (Daga et al. 2016), as well as with environmental and climate changes (Hermanns and Biester 2011, 2013a,b; Hermanns et al. 2013; Biester et al. 2018).

3.2 Mercury in the Nahuel Huapi Catchment

Atmospheric Mercury: Assessments Through Bioindication and Ambient Concentration Monitoring

Lichens have been extensively used as bioindicators of atmospheric pollution since they can store nonessential elements from the surrounding environment with little to negligible effects on their biological functions (Garty 2001; Bargagli et al. 2016). Atmospheric Hg bioindication studies in NHNP using native lichen species have

reported THg levels in thalli ranging from 0.06 to 1.38 μg g^{-1} dry weight (DW), reflecting both natural and human-related Hg sources (Ribeiro Guevara et al. 1995, 2004; Bubach et al. 2012, 2014). Translocation experiments initiated with thalli of native lichen species from pristine areas of the park and transplanted to urban settings in San Carlos de Bariloche city showed a substantial increase in their natural (background) THg levels (from ≤0.107 μg g^{-1} DW to ≤0.280 μg g^{-1} DW), reflecting the influence of Hg emissions due to local human activity (Bubach et al. 2001).

The first instrumental assessment of atmospheric mercury levels in North Patagonia was performed in 2007, during an international survey that included measurements of gaseous elemental mercury (GEM) in different sites of South America. During this campaign, GEM concentrations were measured on different transects within NHNP, using a portable cold vapor atomic absorbance system (Lumex RA-915M). GEM concentrations ranged from 1 to 18 ng m^{-3}, displaying a large spatial variability with high levels (~15 to ~18 ng m^{-3}) close to the Traful area and to the volcanic complex Puyehue-Cordón Caulle (PCCVC), and also in the adjacencies of the Huemul branch of Nahuel Huapi lake (~10 ng m^{-3}). Other sectors of the park showed much lower GEM levels, ranging between ~1 and ~3 ng m^{-3} (Fig. 8.2a) (Horvat and Kotnik 2007; Higueras et al. 2014).

The continuous monitoring of atmospheric mercury in NHNP started in 2011, when the Global Mercury Observation System (GMOS: http://www.gmos.eu/) established the EMMA Station (41° 07' S, 71° 25' W; 800 m a.s.l) in the suburbs of San Carlos de Bariloche City. Currently, this station integrates the GOS4M global network (http://www.gos4m.org), a flagship of the Group of Earth Observation (GEO). Gaseous elemental Hg (Hg^0, GEM), oxidized mercury compounds (GOM comprising mostly Hg halides and HgO), and particle-bound mercury (PBM)] are measured using an automated Hg cold vapor atomic fluorescence spectrometer coupled to speciation modules (Tekran Instrument Corp., Canada). High-resolution data of atmospheric Hg obtained from 2012 to 2019 indicated low mean GEM concentrations (0.86 ± 0.16 ng m^{-3}) with a seasonal pattern characterized by the highest level in spring (0.95 ± 0.13 ng m^{-3}) and the lowest in autumn (0.80 ± 0.15 ng m^{-3}). GOM concentration averaged 4.61 ± 4.00 pg m^{-3}, fluctuating seasonally with the highest levels in autumn and the lowest in winter. PBM averaged 3.74 ± 3.41 pg m^{-3}, with the highest mean level recorded in autumn and the lowest in spring. THg and also its fractions (GEM, GOM, and PBM) displayed overall higher concentrations during daytime hours. Total Hg showed a minimum concentration in the early morning, high values from midday toward the afternoon, and overall lower levels during nighttime. The dynamics of the different atmospheric Hg species have been found to be influenced by the direction and speed of the winds as well as by the temperature and humidity (Diéguez et al. 2019). In order to study the influence of atmospheric transport from local and regional sources in the sector of NHNP covered by the EMMA station, the hybrid single-particle Lagrangian Integrated Trajectory model (HYSPLIT) was applied to calculate air mass backward trajectories (BWT). This analysis indicated that atmospheric Hg concentrations in NHNP are simultaneously affected by local and regional sources (forest fires and volcanoes). Noteworthy,

lower concentrations were recorded with the inflow of clean oceanic air masses corresponding to long-range transport. A Potential Source Contribution Function analysis (PSCF) showed that emissions in the marine boundary layer from remote areas in the Pacific Ocean are also sources of GEM and GOM. Thus, the results obtained through the monitoring of atmospheric Hg inside NHNP confirmed the influence of volcanic sources and forest fires previously reported in studies based on lake sediment sequences. Low levels of atmospheric Hg, such as those recorded coinciding with the influx of clean air masses from the Pacific Ocean and corresponding to long-range transport, indicate the influence of circulating Hg in the global atmosphere (Diéguez et al. 2019).

Mercury in Vegetation and Soils

The distribution of Hg in the landscape has been found to correlate to latitude, annual precipitation, soil organic matter, leaf area, and vegetation greenness. Studies at landscape scale have shown that forested watersheds and their drainage network (including riverine and lacustrine sediments) show comparatively higher concentrations of Hg^{2+} compared to other ecosystems. Forest vegetation and soils store huge quantities of Hg and, thus, largely determine the Hg levels at the watershed scale (Fleck et al. 2016; Obrist et al. 2018). In particular, soil compartments have been extensively studied to assess historical atmospheric deposition because soil is the most important terrestrial repository of contaminants. In mountain regions, which are prone to atmospheric deposition, soil Hg concentrations are the result of the natural background due to local mineral composition and from natural and anthropogenic atmospheric inputs (Zhang et al. 2013). Vegetation patterns largely determine Hg levels in soils due to the importance of the plant-funneled Hg^0 deposition process, being atmospheric deposition to forests up to four times higher than wet deposition in open sites (Grigal 2002). Consequently, forest soils show much higher Hg levels than shrublands and deserts in which the smaller contribution of the vegetation and higher reemission of Hg^0 lead to lower Hg accumulation. Nevertheless, accumulation and retention of Hg in soils are determined by several intrinsic variables such as morphology and genesis, texture, pH, organic matter (OM) content, and stability (reviewed in Obrist et al. 2018).

Soils of Andean Patagonia display original features due to the accumulation of volcanic ash resulting from the intense volcanic activity of the region and the presence of temperate-cold humid forests (Pereyra and Bouza 2019). Andisols have scarce differentiation of their horizons and a high content of allophanes (amorphous clays derived from the weathering of volcanic glass), showing high capacity for water retention, OM stabilization, P retention, and pH buffering (Mazzarino et al. 1998; Pereyra and Bouza 2019). Little is known about the occurrence and dynamics of Hg in Patagonian soils. In this sense, a first evaluation of Hg levels in connected environmental matrices (including soils) within NHNP focused in the subcatchment of Brazo Rincón (BR, 40° 44’ S, 71° 46’ W), a western branch of Nahuel Huapi lake situated at ~30 km southeast of the active PCCVC (Fig. 8.2a). This lake branch

(surface: ~11 km^2, maximum depth: 100 m) drains a catchment of ~227 km^2 and displays a high watershed to lake area ratio (20/6). The landscape is characterized by steep slopes covered (>70%) by a dense forest of deciduous and evergreen *Nothofagus* spp. Previous studies showed the presence of high THg levels in environmental compartments and aquatic biota of this subcatchment, reaching concentrations found in contaminated sites worldwide, and contrasting with much lower levels recorded in other locations of the park (Rizzo et al. 2011, 2014). These conditions indicate that the subcatchment of BR can be considered as a hotspot of Hg within NHNP, encouraging further studies focused on soils, vegetation, and water bodies draining to BR. Total Hg concentrations measured in rainfall samples collected in the BR catchment varied between 21 and 27 ng L^{-1}, suggesting a minor contribution of wet atmospheric deposition. Soil profiles under the canopies of *Nothofagus* spp. showed scarce development below the upper volcanic ash layer deposited during the 2011–2012 PCCVC eruption and characterized by the occurrence of O, A, and 2A horizons. The C horizon which separates the A and 2A horizons corresponded to the weathered parent material with tephra characteristics that correlated with the PCCVC eruption of 1960 and the Calbuco volcano eruption of 1961. OM content in the O horizons ranged from 14.2 to 25.3 %, and THg concentrations varied from 19 to 106 ng g^{-1}, with THg:OM ratios ranging from 1.3 to 4.6 (Rizzo et al. submitted). A direct relationship between THg and OM concentrations in the O horizon and with the altitude suggests that altitudinal vegetation patterns could drive THg levels in soils. The native forest is characterized by the dominance of the evergreen *Nothofagus dombeyi* at the piedmont (from ~670 to ~900 m.s.s.l.) and the prevalence of the deciduous *N. pumilio* above 900 m a.s.l. These tree species have distinct litterfall and throughfall contributions of Hg to soils due to species-specific Hg storage and timing of leaf fall. In fact, the foliage of the evergreen species *N. dombeyi* has been found to contain higher THg concentrations (19 to 190 ng g^{-1}) compared to the deciduous *N. antarctica* (17 to 45 ng g^{-1}) (Juárez et al. 2016). Evergreen foliage incorporates Hg yearlong, while deciduous foliage incorporates it during the growing season, releasing differential amounts of Hg to soils through litterfall (leaf turnover and/or leaf fall) and throughfall, showing also seasonal differences in the contribution (Bushey et al. 2008).

Future studies of Hg dynamics in the area should evaluate key processes such as the uptake of atmospheric Hg by the forest vegetation, its storage, and the factors involved in its transference to soils and aquatic ecosystems, pathways underrepresented in the research carried out in the region up to the moment.

Mercury in Freshwaters

Mercury is naturally present in waters at very low levels. As it has a high tendency to adsorb on surfaces, a large proportion in the water phase is attached to suspended particles, which play an important role in the transport of Hg in aquatic systems. Inorganic Hg tends to bind strongly to mineral particles and detrital OM, whereas CH_3Hg tends to be more strongly associated with biogenic particles, including

organisms such as bacteria, algae, and phytoplankton. Settling of this particulate matter is considered a major delivery mechanism to the sediments which are thus considered as a sink for Hg (Ullrich et al. 2001; Ravichandran 2004; Gallorini and Loizeau 2021). An important part of the biogeochemical cycle of Hg in aquatic systems involves its reemission from the sediments to the water column, which may be substantial in shallow lakes and running waters (Yang et al. 2020).

Between 2011 and 2020, Hg levels in streams and lakes of different areas of NHNP have been surveyed along with physical and chemical water variables, including the concentration and quality of DOC and suspended solids, in order to evaluate Hg availability and fractionation taking into account the THg:DOC ratios. DOC concentration affects the supply and bioavailability of Hg in aquatic systems, and the THg:DOC ratio determines the sorption of Hg to particles and dissolved compounds, which in turn influence the kinetics of Hg reduction, the transference of Hg to the sediments, and its entry to food webs (Ravichandran 2004; Bravo and Cosio 2019; Branfireun et al. 2020; Gèntes et al. 2021). Until now, total mercury (THg) and speciated Hg levels (Hg^{2+}, Hg^0, and CH_3Hg) have been assessed in different water bodies of NHNP alternatively through cold vapor atomic absorption and fluorescence spectroscopy (CVAAS and CVAF, respectively) (Soto Cárdenas et al. 2018a and references therein). In a survey of aquatic systems performed at the western sector of the BR, during the eruption of the PCCVC in 2011, high THg levels were detected, ranging from 41 to 363 ng L^{-1} in streams and from 16 to 268 ng L^{-1} in lakes. High Hg availability in these systems was indicated by the large THg:DOC ratios (from 60 to 1205 ng mg^{-1} in streams and from 52 to 785 ng mg^{-1} in lakes) (Table 8.1, Soto Cárdenas et al. 2018a). Noteworthy, much lower THg concentrations (0.7–9.4 ng L^{-1}) were recorded in the water column of BR a few years afterward (2018 to 2020) suggesting that the large inputs of Hg deposited in the catchment during the last eruption of PCCVC may have been stabilized in the terrestrial environment and buried in lake sediments. In fact, the low THg levels detected in porewater (<0.5–22.6 ng L^{-1}; Pérez Catán et al. 2016) could be taken as an indication of Hg immobilization in the sediments. In the eastern section of the park, levels of THg were much lower (0.48–52 ng L^{-1} in streams and 0.02–56 ng L^{-1} in lake water), resulting in THg:DOC ratios from 0.8 to 105 ng mg^{-1} and from 0.005 to 55 ng mg^{-1}, respectively (Soto Cárdenas et al. 2018a; Arcagni et al. 2019).

High THg concentrations have been detected also in other sites of Nahuel Huapi lake influenced by human-associated pollution. THg concentrations as high as 1750 (±160) ng L^{-1} and 640 (±20) ng L^{-1} were recorded in surface waters of Nahuel Huapi lake in front of the outlet of the sewage treatment plant of San Carlos de Bariloche City and in Villa la Angostura City port, respectively (Pérez Catán et al. 2003).

In natural waters from the BR catchment, THg concentrations measured after the last eruption of the PCCVC in 2011 (Table 8.1) are among the highest concentrations reported in the literature for pristine sites and comparable to those found in impacted environments (Shanley et al. 2008; Kocman et al. 2011). Hg^{2+} was the

Table 8.1 Water parameters (mean ± SD) of aquatic systems of Brazo Rincón catchment (Lake Nahuel Huapi)

	Streams		Lake Pire		Brazo Rincón (Lake Nahuel Huapi)			
	Mean ± SD	Range	Mean ± SD	Range	Mean ± SD	Water column	Upper layers	Deeper layers
DOC (mg L^{-1})	0.60 ± 0.23	0.21–1.02	0.48 ± 0.01	0.41–0.55	0.36 ± 0.06	0.31–0.51	0.32–0.51	0.31–0.33
TSS (mg L^{-1})	7.07 ± 6.72	0.027–22.067	3.7 ± 0.7	3.22–4.22	1.11 ± 0.71	0.44–2.79	0.50–2.79	0.44–1.46
THg (ng L^{-1})	146.08 ± 109.70	40.7–363.0	78.4 ± 20.9	63.6–93.1	126.4 ± 79.5	16.8–268.0	114.0–268.0	16.8–35.6
PTHg (ng L^{-1})	29.1 ± 19.5	7.1–67.3	43.2 ± 6.6	38.5–47.8	40.1 ± 28.7	0.3–76.6	46.9–76.6	0.3–0.9
FTHg (ng L^{-1})	117.0 ± 95.0	14.6–303.8	35.2 ± 14.3	25.1–45.3	86.4 ± 55.1	16.5–202.1	62.5–202.1	16.5–35.3
log K_d	4.96 ± 0.61	3.94–6.03	5.6 ± 0.04	5.5–5.6	5.34 ± 0.67	4.03–5.93	5.54–5.93	4.03–4.70
Hg^{2+} (ng L^{-1})	145.2 ± 109.5	40.4–362.1	77.9 ± 20.9	63.2–92.8	123.1 ± 77.4	16.7–262.8	110.7–262.9	16.7–35.5
CH_3Hg (ng L^{-1})	0.126 ± 0.09	0.04–0.30	0.12 ± 0.04	0.09–0.15	0.06 ± 0.05	0.01–0.16	0.05–0.16	0.01–0.02
THg:DOC (ng mg^{-1})	324.52 ± 349.58	60.3–1204.4	172.3 ± 79.0	116.5–228.2	348.1 ± 226.7	51.9–784.8	279.6–784.8	51.9–106.8
CH_3Hg:DOC (ng mg^{-1})	0.26 ± 0.26	0.06–0.83	0.27 ± 0.14	0.17–0.37	0.16 ± 0.10	0.03–0.31	0.12–0.31	0.03–0.06
Hg^0 (ng L^{-1})	0.80 ± 0.37	0.22–1.33	0.25 ± 0.86	0.19–0.32	3.33 ± 2.46	0.12–6.63	3.14–6.63	0.12–0.14
%Hg^{2+}	99.20 ± 0.37	98.65–99.76	99.50 ± 0.19	99.36–99.63	97.79 ± 1.31	96.14–99.59	96.14–98.09	99.14–99.59
%Hg^0	0.71 ± 0.37	0.18–1.31	0.35 ± 0.20	0.20–0.50	2.16 ± 1.32	0.38–3.81	1.82–3.81	0.38–0.74
%CH_3Hg	0.10 ± 0.05	0.04–0.21	0.15 ± 0.01	0.14–0.16	0.05 ± 0.03	0.03–0.12	0.03–0.09	0.03–0.12

DOC (dissolved organic carbon), TSS (total suspended solids). Mercury species: THg (total Hg), PTHg (total particulate Hg), FTHg (filtered total Hg), CH_3Hg (methyl Hg), Hg^{2+} (ionic Hg), Hg^0 (dissolved gaseous elemental Hg)], log Kd (partitioning coefficient between the particulate PTHg and aqueous phase FTHg (Kd = PTHg/FTHg), THg:DOC and CH_3Hg:DOC ratios (THg and CH_3Hg relative to DOC, respectively). Upper lake layers (0–60 m), deeper lake layers (70–90 m)

prevailing species in all waters, accounting for up to 99.8 % of THg. CH_3Hg levels were down to 0.12% of THg. This probably relates to the combination of high precipitation, low temperature, and steep slopes that promote rapid runoff preventing Hg methylation in soil and streambeds (Soto Cárdenas et al. 2018a). DOC levels were low, fluctuating between 0.31 and 1.02 mg L^{-1}. THg:DOC ratios ranged from 50 to 1204, indicating high Hg^{2+} availability, with high partitioning coefficients (log Kd: Hg availability for binding particles). Overall, low DOC levels and high Hg^{2+} concentrations in these systems promote a high adsorption of Hg^{2+} to abiotic and biotic particles. In fact, particulate THg (PTHg) took values up to 76.6 ng L^{-1} and was associated with inorganic particles in the streams and with phytoplankton in the lakes (Soto Cárdenas et al. 2018a).

In streams, Hg fractionation and speciation related directly with DOM terrestrial signatures (high molecular weight and aromatic DOM), indicating coupled Hg-DOM inputs from the catchment. In BR, DOM quality and photochemical and biological processing were found to determine Hg fractionation, speciation, and vertical levels. Dissolved gaseous Hg (DGM) reached higher values in BR (up to 3.8%), particularly in upper layers likely due to photochemical weathering resulting in the photolysis of Hg-DOM complexes and reduction of Hg^{2+} (Fig. 8.1; Soto Cárdenas et al. 2018a).

Box 8.1 Information

Trends arising from different Hg studies in aquatic systems of Nahuel Huapi National Park

(i) Hg^{2+} comprises up to 98% of the THg concentrations the water phase, while those of CH_3Hg are below 3%
(ii) THg levels in waters directly relate with terrestrial DOC signatures, particularly in streams, indicating lateral transport of tied DOC-Hg inputs from the terrestrial environment
(iii) THg:DOC ratios in waters are high in a global context, indicating remarkable high Hg availability (mostly as Hg^{2+})
(iv) High THg levels coincide with chlorophyll *a* peaks in the water column of lakes, indicating high Hg levels stored in phytoplankton, whereas in streams Hg is adsorbed to inorganic particles
(v) CH_3Hg levels in streams relate with allochthonous DOM inputs indicating a terrestrial source, while in lakes, the higher levels in deep layers can be attributed to diffusion from and resuspension of sediments
(vi) In the depth profile of lakes, internal processing (photo- and biodegradation) tracked through optical DOC proxies, was found to favor the production of dissolved gaseous mercury (Hg^0). Particularly, the optically thin water column of deep ultraoligotrophic lakes promotes high light penetration and photolytic transformations of Hg

Mercury in Lacustrine Sediments

Mercury deposited directly on the lake surface is rapidly scavenged by settling particles and sequestered to the sediments, and Hg deposited on the watershed is transported to the lakes mainly bound to OM and fine-grained mineral matter (Kainz and Lucotte 2006; Cooke et al. 2020 and references therein). Its cycling and distribution between the sediment and the water phase can be physically, chemically, and/or biologically mediated and, therefore, may be influenced by several factors such as pH, dissolved oxygen concentration, temperature, redox conditions, nutrients, and complexing agents (Ullrich et al. 2001; Ravichandran 2004; Bravo and Cosio 2019; Branfireun et al. 2020).

The prevalence of inorganic and organic Hg^{2+} complexes, as well as redox processes involving Hg^{2+} and Hg^0, and the partitioning of Hg between particulate, aqueous, and gaseous phases are important in the sediments (Beckers and Rinklebe 2017). Methylation of Hg^{2+} can occur in the sediments and in the water column of stratified lakes, with higher net methylation rates occurring mainly at the oxic/anoxic interface (reviewed in Dranguet et al. 2017; Bravo and Cosio 2019; Gallorini and Loizeau 2021). Moreover, CH_3Hg from terrestrial sources may contribute to the pool of Hg present in riverine and lacustrine sediments. In this sense, lake sediments dominated by OM derived from the catchment show higher CH_3Hg concentrations but lower rates of in situ methylation, in contrast with sediments dominated by autochthonous OM (Branfireun et al. 2020 and references therein).

In NHNP, differences in Hg background levels in sediment cores from different lakes were associated with lake productivity. Background mercury levels in sediment cores obtained in Bahía López (BL; Nahuel Huapi lake), Moreno West, and Traful lakes ranged from <0.08 to 0.210 (± 0.044) μg g^{-1} in preindustrial times, and twice as much in modern times. Higher Hg concentrations were detected in sediment cores of lakes El Trébol (7.02 ± 0.84 μg g^{-1}), Escondido (2.80 ± 0.36 μg g^{-1}), and Morenito (1.52 ± 0.32 μg g^{-1}). These lakes are small, shallow (maximum depth <12 m), and closed systems and display higher productivity than deep lakes of the area (OM between 22.5 and 26.5%). In the deep, ultraoligotrophic Nahuel Huapi lake branch BR, the highest THg concentration was recorded in the uppermost layer (1.10 ± 0.27 mg g^{-1}) corresponding to the period 1987–1994, displaying a positive correlation with OM (Ribeiro Guevara et al. 2002, 2003, 2005).

Studies focused on the THg content in suspended particles in the water column of different sites in Nahuel Huapi lake collected along with sediment cores indicated that both OM and Hg inputs from the catchment are highly seasonal and variable depending on the precipitation pattern. In this lake, the concentration of Hg in the suspended load was higher in the wettest sector (BR) compared to the dryer sites Puerto Cisne (PC) and the coast of San Carlos de Bariloche City (BRC) (Ribeiro Guevara et al. 2002), suggesting that the steep precipitation gradient observed in the area reflects in higher deposition and mobilization of materials from the landscape at the wetter BR catchment.

The production of CH_3Hg from Hg^{2+} in lake sediments was evaluated through laboratory experiments with the short-lived radioisotope 197Hg ($t^{1/2}$ = 64.14 h)

using surface sediments and biofilms from different lakes of NHNP (Pérez Catán et al. 2004, 2007; Ribeiro Guevara et al. 2004, 2009). Mercury methylation potentials showed a seasonal trend due to variations in biotic and abiotic contributions. An increased abiotic contribution was observed during winter, at a moment of low biological productivity. Slightly higher methylation potentials were recorded in autumn, possibly associated with fresh terrestrial inputs due to increased seasonal runoff (Pérez Catán et al. 2009). Such inputs may include CH_3Hg produced in the terrestrial environment (soil) and could promote changes in the concentration and quality of the OM and nutrient pools, influencing Hg methylation processes in lakes (Bravo et al. 2017). Experiments on mercury methylation using radiolabeled Hg^{2+} showed that top sediments and rocks yielded lower methylation rates than autotrophic and heterotrophic biofilms, stressing the importance of biotic production of CH_3Hg (Pérez Catán et al. 2011).

4 Mercury Trophodynamics in Lakes

Mercury entry, speciation, cycling, and accumulation in food webs are influenced by a multiplicity of variables, such as levels of Hg^{2+} in the dissolved phase, DOM concentration and quality, levels of $Hg^{2+}$and CH_3Hg at the base of the food web, activity of microbial methylators, among others. In addition, several ecological features such as primary productivity, habitat use, bioenergetics, and food web structure affect the efficiency of Hg uptake and its biomagnification (Arcagni et al. 2018; Eagles-Smith et al. 2018; Braaten et al. 2020; Chételat et al. 2020). In lakes, the habitat where fish feed can affect the amount of Hg that they accumulate. In large, deep lakes with extended pelagic zones, fish belonging to the same trophic position feeding in the pelagic habitat usually present higher Hg than fish foraging in the littoral (Chételat et al. 2011; Gèntes et al. 2021, and references therein). In contrast, in some lakes, fish feeding in the littoral habitat show higher Hg concentrations than pelagic-feeding fish (e.g., Chumchal et al. 2008; Finley et al. 2016; Hanna et al. 2016). Differential bioaccumulation of Hg between pelagic and benthic habitats may be related to Hg concentrations in prey and/or with differences in bioenergetic processes at the base of the food web (Kidd et al. 2003; Karimi et al. 2016).

The structure of pelagic food webs of deep Andean Patagonian lakes is simple and characterized by high endemicity and low diversity and abundance of organisms (Modenutti et al. 1998, 2010; Chap. 3). Limiting nutrient and C concentrations as well as high solar radiation and low temperature are the main challenges faced by pelagic communities. The picoplanktonic fraction is dominated by heterotrophic bacteria and picocyanobacteria (Callieri et al. 2007; Izaguirre et al. 2014; Soto Cárdenas et al. 2014, 2019; Gerea et al. 2019). Phytoplankton is mainly composed by nanoplanktonic flagellates (*Chrysochromulina parva*, *Rhodomonas lacustris*, etc.), dinoflagellates (*Gymnodinium* spp., *Dynobryon* spp., *Peridinium* spp.), and diatoms (i.e., *Aulacoseira granulata*, *Rhizosolenia eriensis*, and *Cyclotella stelligera*) (Diaz et al. 1998; Modenutti et al. 1998; Queimaliños et al. 1999, 2002; Soto

Cárdenas et al. 2014). Mixotrophy (photosynthesis + phagotrophy) is a common trait to different species of flagellates and ciliates (Hansen et al. 2019), and, in Andean lakes, this nutrition mode allows compensating the C and nutrient limitation through bacteria consumption and/or through the photosynthesis of endosymbiotic algae (Queimaliños et al. 1999; 2002; Modenutti et al. 2010; Gerea et al. 2017). The zooplankton community is composed of ciliates, rotifers, and crustaceans including cladocerans (*Bosmina longirostris*, *Ceriodaphnia dubia*, and the less abundant *Daphnia* sp.), calanoid (*Boeckella gracilipes*), and cyclopoid copepods (Modenutti et al. 1998; Arcagni et al. 2015).

Benthic food webs are also simple and in littoral areas characterized by the presence of the submerged macrophytes *Myriophyllum* sp. and *Nitella* sp., the emergent sedge *Schoenoplectus californicus*, and periphyton communities dominated by diatoms. The littoral zoobenthos assemblages are usually composed of insect larvae and nymphs of Trichoptera, Ephemeroptera, Plecoptera, Odonata, and Diptera (fam. Chironomidae, midges); *Chilina* sp. (snail) and *Diplodon chilensis* (mussel) mollusks; *Aegla* spp. (crab), *Samastacus spinifrons* (crayfish) and *Hyalella* sp. (amphipod) crustaceans, and annelids (hirudineans and oligochaetes) (Modenutti et al. 1998; Arcagni et al. 2013a, 2015). Fish assemblages include five native species, *Percichthys trucha* (creole perch), *Galaxias maculatus* (small puyen), *G. platei* (big puyen), *Olivaichthys viedmensis* (velvet catfish), and *Odontesthes hatcheri* (Patagonian silverside), and three introduced species of salmonids, *Salmo trutta* (brown trout), *Oncorhynchus mykiss* (rainbow trout), and *Salvelinus fontinalis* (brook trout) (Arcagni et al. 2015, and references therein).

Pelagic microbial assemblages of Andean lakes are included in the plankton fractions with higher THg levels (Table 8.2). Heterotrophic and autotrophic bacteria, flagellates (*Gymnodinium* spp.), and mixotrophic ciliates (*Stentor araucanus* and *Ophrydium naumanni*) incorporate substantial amounts of dissolved Hg^{2+} passively (adsorption) and actively (bacteria consumption or attachment), differing in Hg internalization and thus, in their potential for Hg transfer (Soto Cárdenas et al. 2014, 2018b, 2019). Morphological features of protists such as surface area and surface to volume ratio, as well as the concentration and quality of DOC control their passive uptake (Diéguez et al. 2013; Soto Cárdenas et al. 2014). Active incorporation of Hg^{2+} depends on bacteria consumption in the mixotrophic ciliates, or on bacteria association to surface. Therefore, Hg^{2+} accumulated by pelagic protists can transfer to higher trophic levels through their consumption by plankton and fish, can regenerate to the dissolved phase, and/or be transferred within the water column and to the sediments by vertical movements (diel vertical migration), excretes and particle sinking (debris, resting stages, etc.) (Chiaia-Hernandez et al. 2013; Aydin et al. 2015, Soto Cárdenas et al. 2018b, 2019). In aquatic food webs, microbes have a chief influence on Hg pathways and speciation, since they can scavenge different Hg species, reduce Hg^{2+}, oxidize Hg^0 and produce and degrade CH_3Hg (Gregoire and Poulain 2014, 2018; Bravo and Cosio 2019). The conversion of inorganic Hg^{2+} to CH_3Hg in the environment is mostly carried out by microbial assemblages present in anaerobic sediments, saturated soils, anoxic bottom waters, and also in oxygen-deficient microenvironments (biofilms and microbial flocks) in oxygenated

Table 8.2 Range, mean, and standard deviation of total mercury (THg) and methyl Hg (CH_3Hg) concentrations in biota from Lake Nahuel Huapi and surrounding sites (BL, Bahía Lopez; BR, Brazo Rincón; DH, Dina Huapi; BRC, San Carlos de Bariloche City)

Taxa	Site	THg (μg g^{-1})		CH_3Hg (μg g^{-1})		Reference
		Mean (± SD)	Range	Mean (± SD)	Range	
FISH						
Galaxias maculatus (small puyen)	BL	0.169 ± 0.077 (11, 30)	0.031–0.286[a]	0.139 ± 0.041 (5, 19)	0.089–0.188	1, 2, 3
	BR	0.278 ± 0.118 (23, 73)	0.077–0.650[a]	0.184 ± 0.079 (7, 48)	0.027–0.272	1, 2, 3
	DH	0.257 ± 0.264 (17, 48)	0.040–1.00[a]	0.051 ± 0.016 (6, 20)	0.024–0.071	1, 2, 3
Galaxias platei (big puyen)	BR	0.673 ± 0.454 (8, 8)	0.298–1.72[b]	0.745 ± 0.444 (6, 6)	0.354–1.76	1, 2
	DH	1.43 (1, 1)		–	–	1
Olivaichthys viedmensis (velvet catfish)	BL	0.499 (1, 1)		0.447 (1, 1)	–	1, 2
	DH	0.719 (1, 1)		0.748 (1, 1)	–	1, 2
Oncorhynchus mykiss (rainbow trout)	BL	0.087 ± 0.047 (7, 7)	0.039–0.180[b]	0.082 ± 0.041 (7, 7)	0.033–0.157	1, 2
	BR	0.166 ± 0.063 (5, 5)	0.105–0.264[b]	0.147 ± 0.073 (4, 4)	0.106–0.257	1, 2
	DH	0.090 ± 0.063 (10, 10)	0.027–0.252[b]	0.049 ± 0.020 (8, 8)	0.019–0.082	1, 2
O. mykiss, juveniles	BL	0.083 ± 0.016 (6, 6)	0.066–0.102[b]	0.066 ± 0.005 (4, 4)	0.060–0.072	1, 2
	DH	0.146 ± 0.177 (3, 3)	0.041–0.350[a]	0.022 (1, 1)	–	1, 2
Percichthys trucha (creole perch)	BL	0.706 ± 0.296 (9, 9)	0.137–1.09[b]	0.714 ± 0.390 (8, 8)	0.145–1.27	1, 2
	BR	1.13 ± 0.56 (13, 13)	0.573–2.33[b]	1.08 ± 0.41 (11, 11)	0.559–1.83	1, 2
	DH	0.430 ± 0.317 (5, 5)	0.090–0.761[b]	0.070 ± 0.01 (2, 2)	0.063–0.076	1, 2
Salmo trutta (brown trout)	BL	0.256 ± 0.174 (2, 2)	0.133–0.379[b]	0.235 ± 0.186 (2, 2)	0.105–0.364	1, 2
	BR	0.216 ± 0.110 (23, 23)	0.053–0.467[b]	0.213 ± 0.144 (13, 13)	0.054–0.536	1, 2
	DH	0.241 (1, 1)		–	–	1
S. trutta, juveniles	BR	0.259 ± 0.051 (5, 13)	0.206–0.335[a]	0.243 ± 0.033 (3, 7)	0.220–0.280	1, 2
Macroinvertebrates						
Aegla sp. (crabs)	BL	0.246 ± 0.172 (13, 84)	0.110–0.786[b]	0.096 ± 0.014 (2, 9)	0.086–0.106	1, 2
	BR	0.592 ± 0.722 (12, 63)	0.168–2.72[b]	0.223 ± 0.026 (3, 17)	0.198–0.249	1, 2

(continued)

Table 8.2 (continued)

Taxa	Site	THg (μg g^{-1})		CH_3Hg (μg g^{-1})		Reference
		Mean (± SD)	Range	Mean (± SD)	Range	
Chilina sp. (snails)	BL	0.564 ± 0.401 (12, 66)	0.115–1.04[b]	0.018 ± 0.003 (2, 20)	0.016–0.019	1, 2
	BR	0.166 ± 0.064 (38, 188)	0.069–0.296[b]	–	–	1
Diplodon chilensis (mussel)	BL	0.160 ± 0.118 (15, 77)	0.063–0.560[b]	0.018 ± 0.01 (5, 28)	0.013–0.031	1, 2
Hyalella sp. (amphipods)	BL	0.424 ± 0.033 (2, 22)	0.400–0.447[b]	–	–	1
	BR	0.346 ± 0.163 (4, 123)	0.234–0.584[c]	–	–	1
Insect larvae (various spp.)	BL	0.374 ± 0.496 (26, 195)	0.042–1.15[c]	0.007 ± 0.001 (2, 24)	0.0062–0.0081	1, 2
	BR	0.326 ± 0.192 (29, 335)	0.062–0.806[c]	0.034 ± 0.004 (3, 86)	0.031–0.039	1, 2
Samastacus spinifrons (crayfish)	BL	0.113 ± 0.040 (15, 30)	0.058–0.191[b]	0.083 ± 0.020 (5, 14)	0.061–0.109	1, 2
	BR	0.480 ± 0.251 (18, 33)	0.185–1.10[b]	0.561 ± 0.448 (6, 9)	0.165–1.43	1, 2
	DH	0.123 ± 0.086 (6, 8)	0.038–0.249[b]	0.080 ± 0.058 (4, 6)	0.029–0.136	1, 2
Aquatic Communities						
Biofilm	BL	0.4454 (1)	–	–	–	1
	BR	0.128 ± 0.064 (2)	0.083–0.173[d]	–	–	1
Plankton, fraction 10–53 μm	BL	18.4 ± 14.6 (2)	8.07–28.7[d]	–	–	1, 2
	BR	81 ± 123 (4)	0.930–260[d]	–	–	1, 2
	DH	26.4 ± 1.6 (2)	25.2–27.1[d]	–	–	1, 2
Plankton, fraction 53–200 μm	BL	4.76 ± 4.44 (5)	0.372–9.81[d]	0.0057 (1)	–	1, 2, 3
	BR	7.14 ± 10.92 (6)	0.340–31.2[d]	0.004 ± 0.001 (3)	0.003–0.006	1, 2, 3
	DH	8.37 ± 7.77 (4)	1.47–19.1[d]	0.0039 (1)	–	1, 2, 3
Plankton, fraction > 200 μm	BL	3.82 ± 6.71 (5)	0.344–15.8[d]	0.012 ± 0.02 (2)	0.011–0.013	1, 2, 3
	BR	1.88 ± 2.71 (10)	0.131–9.56[d]	0.016 ± 0.009 (4)	0.009–0.029	1, 2, 3
	DH	10.1 ± 16.3 (6)	1.00–43.1[d]	0.130 ± 0.174 (2)	0.007–0.253	1, 2, 3

(continued)

Table 8.2 (continued)

Taxa	Site	THg (μg g^{-1})		CH_3Hg (μg g^{-1})		Reference
		Mean (± SD)	Range	Mean (± SD)	Range	
Tree leaves						
Submerged tree leaves debris (various spp.)	BL	0.085 ± 0.045 (6)	0.038–0.144[e]	–	–	4
Tree leaves from the canopy (various spp.)	BL	0.056 ± 0.026 (9)	0.0300–0.119[e]	–	–	4
	BR	0.052 ± 0.043 (15)	0.016–0.174[e]	–	–	4
Lichens						
Candelaria vitellina (crustose areolate lichen)	BRC	–	1.65–2.67[f]	–	–	5, 6
	BRC	–	0.28–0.92[f]	–	–	5, 6
Hypotrachyna brevirhiza (foliose lichen)	BRC	–	1.02–1.51[f]	–	–	5, 6
	BRC	–	0.30–0.85[f]	–	–	5, 6
Physcia adscendens (hooded rosette lichen)	BRC	–	0.18–2.81[f]	–	–	5, 6
Protousnea magellanica (beard lichen)	BRC	–	0.096–0.280[f]	–	–	5, 7
Usnea sp. (old man's beard)	BR	0.197 ± 0.020	0.09–0.23[f]	–	–	8, 9
	BR	0.669 ± 0.089[f]	–	–	–	5
	DH	0.203 ± 0.015[f]	–	–	–	8, 9

Total Hg and CH_3Hg concentrations are presented on a dry weight basis. Numbers in parentheses indicate the number of samples and organisms analyzed; in the case of plankton, biofilm, and tree leaves, only the number of samples is indicated

References: 1-Arcagni et al. (2017); 2-Arcagni et al. (2018); 3-Rizzo et al. (2014); 4-Juárez et al. (2016); 5- Ribeiro Guevara et al. (2004); 6-Ribeiro Guevara et al. (1995); 7- Bubach et al. (2001); 8- Bubach et al. (2012); 9- Bubach et al. (2014)

[a]no head and guts
[b]muscle
[c]whole
[d]bulk sample
[e]leaves
[f]thalli

surface waters (Lehnherr et al. 2011; Lamborg et al. 2014; Gionfriddo et al. 2016; Bravo and Cosio 2019; Gallorini and Loizeau 2021).

The transference of Hg between abiotic and biotic compartments is a critical aspect to understand and delineate the concentration dynamics in the pelagic (water column) and benthic (bottom) habitats. Soto Cárdenas et al. (2018a) showed that in different aquatic systems from the BR catchment (Nahuel Huapi lake), THg concentrations ranged from moderate to high (16.8–268 ng L^{-1}), with Hg^{2+} as the

predominant Hg species (from 96.1 to 99.6 %), whereas CH_3Hg concentrations were low (from 0.03 to 0.12%) indicating reduced methylation in the catchment and in the aquatic systems despite high Hg availability (Soto Cárdenas et al. 2018a). In BR, most of the THg measured in the plankton was Hg^{2+}, and its concentration decreased abruptly with trophic level, from phytoplankton to zooplankton and small puyen. In turn, the concentration of CH_3Hg was comparatively very low but increased with trophic level (Rizzo et al. 2014; Arcagni et al. 2017). This is due to the fact that at the base of the trophic chain, Hg^{2+} adsorbs to the membrane of algal cells, while CH_3Hg is sequestered in their cytoplasm. Zooplankton digest algal cells readily incorporating their cytoplasmic content and excreting the membranes. In this way, CH_3Hg is more efficiently transferred than Hg^{2+} from phytoplankton to zooplankton grazers (Mason et al. 1995, 1996; Diéguez et al. 2013).

In Nahuel Huapi lake, THg and CH_3Hg concentrations in fish species vary by foraging habitat, increasing with a greater proportion of benthic diet over pelagic diet (Arcagni et al. 2017, 2018). Native creole perch, a predominantly benthic feeder, shows higher THg and CH_3Hg levels in muscle than introduced salmonids such as the more pelagic rainbow trout and the benthopelagic brown trout, although the three species are positioned at the highest trophic level of the food web. The native galaxiid known as big puyen is a benthic feeder positioned at a lower trophic

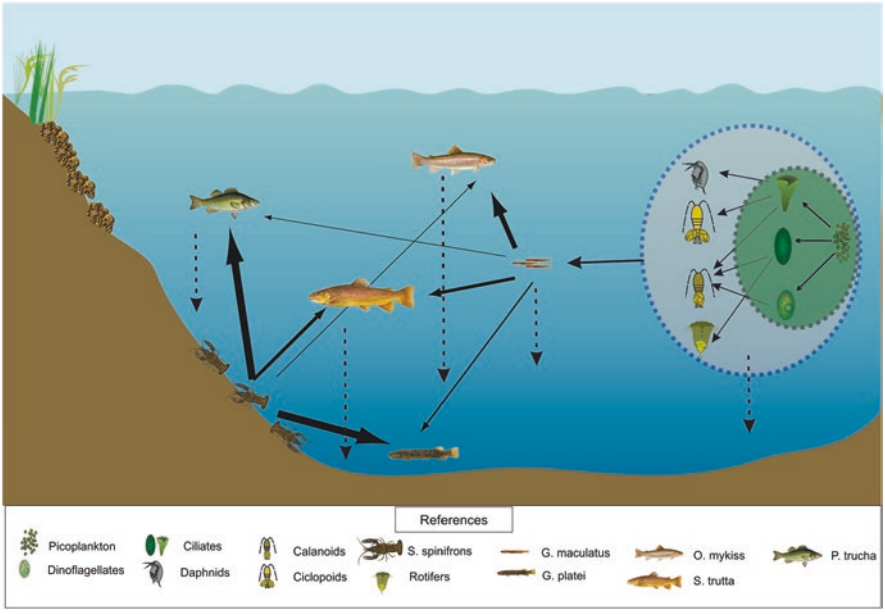

Fig. 8.3 Mercury transference in a typical food web of deep ultraoligotrophic Andean Patagonian lakes. Solid line arrows: CH_3Hg pathway. Dashed line arrows: THg pathway (arrow thickness indicates magnification). Species references: *Percichthys trucha* (creole perch), *Galaxias maculatus* (small puyen), *Galaxias platei* (big puyen), *Salmo trutta* (brown trout), *Oncorhynchus mykiss* (rainbow trout), *Samastacus spinifrons* (crayfish)

level than the creole perch and exotic trout and usually displays higher THg and CH_3Hg concentrations than the salmonids (Table 8.2, Fig. 8.3; Arcagni et al. 2015, 2017, 2018; Juncos et al. 2015).

The distinctive patterns in THg and CH_3Hg bioaccumulation in different fish species could be explained by the niche segregation among native and introduced fish (Juncos et al. 2015) leading to different pathways of Hg transference: a benthic pathway (from sediments to benthic macroinvertebrates and benthivorous fish) and a pelagic pathway (from water, plankton, foraging fish, and piscivorous fish) (Fig. 8.3). At first sight, in deep Andean lakes, the pelagic habitat appears to be a more important source of Hg to the food web than the benthic habitat. THg levels in size-fractionated plankton samples typically decrease from the smaller fraction (10–53 μm) comprising mixotrophic ciliates and dinoflagellates, toward the fraction between 50 and 200 μm composed of large mixotrophic ciliates and rotifers, and the fraction >200 μm made up of copepods and cladocerans (Table 8.2; Arribére et al. 2010; Rizzo et al. 2011, 2014; Arcagni et al. 2013b, 2015, 2017), whereas macroinvertebrates belonging to benthic food webs usually present lower THg concentrations than the different plankton fractions (Table 8.2, Fig. 8.3; Arcagni et al. 2015, 2017). Noteworthy, regardless of the high THg concentrations present in different plankton size fractions, their CH_3Hg concentrations are low, ranging from 0.021 to 6.8% of THg, while those in benthic macroinvertebrates are higher, between 1.5 and 100 %. These levels are reflected in the different Hg pathways mentioned before. In the pelagic trophic chain, *O. mykiss*, which feeds mostly on the planktivorous forage fish *G. maculatus*, shows lower THg and CH_3Hg concentrations than the benthivorous native fishes *P. trucha*, *G. platei*, and *O. viedmensis*; however, over 62% of THg is in the form of CH_3Hg (mean concentration: 81 ± 13%). In the benthic trophic chain, *P. trucha* and *G. platei* feed mostly on crayfish and other macroinvertebrates, resulting in the highest THg and CH_3Hg concentrations in the fish community, with CH_3Hg over 64% (89 ± 12%) of THg. *Salmo trutta*, which relies on *G. maculatus* at smaller sizes and shifts to a diet composed mainly of crayfish at larger sizes, shows intermediate THg concentrations between native fishes and *O. mykiss* and also a high proportion of CH_3Hg (88 ± 11%%) (Fig. 8.3; Juncos et al. 2015; Arcagni et al. 2017, 2018). The trend of increasing CH_3Hg and decreasing Hg^{2+} with trophic level in the pelagic habitat ends in the *G. maculatus–O. mykiss* feeding link, as the latter species displays lower to similar concentrations of Hg^{2+} and similar CH_3Hg level compared to its prey. On the contrary, in the benthic habitat, both THg and CH_3Hg increase with increasing trophic level, from insect larvae and crayfish to *P. trucha* and *S. trutta*, with intermediate CH_3Hg and THg concentrations between *O. mykiss* and *P. trucha*, which has lower Hg^{2+} concentrations than its benthic diet (crayfish) and similar concentrations than its pelagic diet consisting of *G. maculatus* (Fig. 8.3; Arcagni et al. 2017, 2018).

In the sediments, Hg^{2+} can be methylated and taken up by benthic organisms by direct absorption from the porewater and/or from the water passing through the gills during respiration, or indirectly through deposit-feeding, thus reaching benthic predatory fish (Chen et al. 2014 and references therein). Benthic biofilms may also contribute to the CH_3Hg present in benthic feeders, since they are chemically

particular microsites where microbial assemblages include microorganisms with physiological capability for Hg methylation and demethylation (Bravo and Cosio 2019). In fact, biofilms from different Andean Patagonian lakes have been shown to yield high methylation rates, as was discussed in Sect. 4. For example, crayfish, which are polytrophic, may acquire Hg remobilized from the benthic habitat by feeding on small benthic macroinvertebrates and on plant and animal detritus (Rudolph 2002) and then transfer the accumulated Hg to the benthivorous fish, *P. trucha*, or *G. platei* (Fig. 8.3).

5 Perspectives on Mercury Cycling in Andean Patagonian Catchments in a Context of Climate Change

In the northern and central sections of Patagonia, long-term drying and warming trends are driving major hydrological changes affecting headwaters (Masiokas et al. 2008; Garreaud et al. 2013; Barros et al. 2015). Annual and seasonal temperature and precipitation records indicate significant warming and decreasing precipitation since 1912. These climate alterations have been implied as drivers of large-scale changes in Andean Patagonian catchments including the drastic reduction of glacial fields (Chap. 4), the decrease in streams and rivers discharge (Masiokas et al. 2008, 2009; Wilson et al. 2018; Chap. 9), as well as the increase in the frequency of extended wildfires (Mundo et al. 2017). Such climate-related changes may interact with those arising from population and urban expansion at a regional scale and also be influenced by global changes (Chaps. 9 and 11). Hydroclimatic changes stress internal processes of terrestrial, wetland (Chap. 10), and aquatic ecosystems and affect the fluxes of materials from the catchment to the fluvial network. Reduced precipitations and changes in the precipitation pattern lead to changes in the strength of the linkages within the catchment that reflect on the mobilization of materials from the terrestrial environment toward the fluvial network, thus affecting biogeochemical cycling (Battin et al. 2008). Terrestrial inputs drive physicochemical factors controlling the dynamics and function of aquatic communities. Freshwaters of Andean Patagonia, particularly the oligo-/ultraoligotrophic systems, rely tightly and respond rapidly to seasonal terrestrial inputs of C and nutrients (Queimaliños et al. 2012, 2019). Due to the affinity of Hg for organic ligands present in natural OM, the C and Hg biogeochemical cycles are tied (Ravichandran 2004; Lavoie et al. 2019). C and Hg pools are washed from the land by precipitation and runoff, draining through the aquatic network. In fact, changes in the volume, type, and timing of precipitation reflect rapidly in the OM, nutrient, and Hg pools of aquatic systems (Queimaliños et al. 2012, 2019; Rizzo et al. 2014). The magnitude of the impact would depend on the severity of the climate changes and also on the hydrogeomorphic features of the catchment (topography, vegetation cover, soil development, lake morphometry, etc.). If warming and drought patterns sustain over time, aquatic systems will undergo profound changes due to reduced inputs of water and materials

from the catchment affecting several different aspects. Their morphometry may suffer changes due to reduction in depth and surface, implying the loss of littoral zones and related communities. Water retention time in lakes may increase following the reduction of water inputs and water turnover. This would impact water clarity due to DOM photobleaching (Queimaliños et al. 2019; Chap. 3), ultimately enhancing light penetration, particularly the UV wavelengths. In turn, the higher impact of underwater irradiance will increase photochemical processing. Autotrophic and heterotrophic production will likely react to changes in the terrestrial C and nutrients supplies, causing community changes. Moreover, the potential loss of cold-adapted organisms would imply modification of the trophic pathways in which they intervene. All these changes are likely to synergize, affecting the diversity and function of aquatic communities which in turn impact biogeochemical cycling.

Progress in glacial melting due to warming is expected to release large quantities of Hg locked in ice into the atmosphere and downstream ecosystems. However, it is possible that the opposite process will occur and that the glacier-to-vegetation succession already going on will increase the capture of atmospheric Hg, as it has been observed in areas experiencing glacial retreat (Wang et al. 2020). Additionally, the increase of wildfires may also contribute to unlocking Hg stored in natural forests; however, this would depend on concomitant changes in land cover and use due to population growth and urban expansion. In this regard, predictive models of future Hg emissions forecast significant perturbations due to increased wildfire Hg emissions, driven by the changes in climate, land use, and Hg anthropogenic emissions. Modeled scenarios for the 2000–2050 period indicate an increase of Hg emissions by 14% globally and by 18% in South America. The potential increase of Hg in terrestrial ecosystems in response to changes in global Hg anthropogenic emissions and deposition could enhance global Hg emissions due to wildfires. However, this scenario may depend on changes in land use by 2050, since agricultural land expansion in detriment of natural vegetation could decrease global Hg emissions from wildfires (Kumar et al. 2017).

The changes in Hg cycling are expected to be manyfold because Hg stored in ecosystems, processing rates, the lateral transport to aquatic end points, and methylation are climate-sensitive (Obrist et al. 2018). Evidence arising from sediment cores of a remote lake in southern Patagonia (Lake Hambre, Chile) suggests that Hg accumulation over the past 4000 years has been influenced by cyclic changes in climate, total solar irradiance, and lake productivity. The accumulation of Hg was higher in dry periods coinciding with high solar irradiance and lake productivity. In such environmental conditions and assuming low Hg fluxes from the atmosphere to the catchment and to the lake due to drier conditions, Hg burial in the sediments may have reduced the concentration of Hg in the water column as well as the evasion of Hg^0 from the system (Biester et al. 2018).

Given the global reach of Hg pollution, climate-related changes in Hg cycling in the Andean Patagonian region would have to be foreseen in the context of the evolution of global anthropogenic emissions, and, above all, having in mind the stochastic impact of volcanism which is the main source of Hg to regional landscapes. Nevertheless, it can be inferred that the forecasted warming and drying trends would

increase Hg reemission due to enhanced photoreduction processes in terrestrial and aquatic systems, will decrease the lateral transport due to the reduction in the terrestrial-aquatic linkages, and will trigger changes in terrestrial and aquatic methylation due to the reduction of allochthonous C and Hg inputs and changes in microbial communities. Extreme events such as intense rainfall, floods, and droughts, among others, affect South America regardless of the seasons (Marengo et al. 2009). Exceptional floods, which have been forecasted as a component of climate change in the region, could provide unusual pulses of terrestrial materials to aquatic systems, whereas drought would reduce the land-water linkage, shrinking the flow of terrestrial materials within catchments.

These changes would impact the amounts of terrestrial C, nutrients, and Hg reaching the aquatic environment, which in turn drive the uptake, accumulation, and transfer of Hg in aquatic food webs. Moreover, changes in terrestrial subsidies are expected to affect the structure and dynamics of aquatic communities, with potentially profound consequences on the trophic pathways of the biogeochemical cycling of Hg.

References

Ackerman JT, Eagles-Smith CA, Herzog MP et al (2016) Avian mercury exposure and toxicological risk across western North America: a synthesis. Sci Total Environ 568:749–769

AMAP/UNEP (2013) Technical Background Report for the Global Mercury Assessment 2013. Arctic Monitoring and Assessment Programme, Oslo, Norway/UNEP Chemicals Branch, Geneva, Switzerland. p 263

Arcagni M, Campbell LM, Arribére MA et al (2013a) Food web structure in a double-basin ultra-oligotrophic lake in Northwest Patagonia, Argentina, using carbon and nitrogen stable isotopes. Limnologica 43:131–142

Arcagni M, Campbell LM, Arribére MA et al (2013b) Differential mercury transfer in the aquatic food web of a double basined lake associated with selenium and habitat. Sci Total Environ 454–455:170–180

Arcagni M, Rizzo AP, Campbell LM et al (2015) Stable isotope analysis of trophic structure, energy flow and spatial variability in a large ultraoligotrophic lake in Northwest Patagonia. J Great Lakes Res 41:916–925

Arcagni M, Rizzo AP, Juncos R et al (2017) Mercury and selenium in the food web of Lake Nahuel Huapi, Patagonia, Argentina. Chemosphere 166:163–173

Arcagni M, Juncos R, Rizzo AP et al (2018) Species- and habitat-specific bioaccumulation of total mercury and methylmercury in the food web of a deep oligotrophic lake. Sci Total Environ 612:1311–1319

Arcagni M, Soto Cárdenas C, Fajon V et al (2019) Mercury in aquatic systems of Nahuel Huapi National Park: a natural biogeochemical hotspot in northern Patagonia. Abstracts of the 14th international conference on mercury as a global pollutant. Krakow, Poland 8-13 September

Arribére M, Diéguez MC, Ribeiro Guevara S et al (2010) Mercury in an ultraoligotrophic North Patagonian Andean lake (Argentina): concentration patterns in different components of the water column. J Environ Sci 22:1171–1178

Aydin H, Yürür EE, Uzar S et al (2015) Impact of industrial pollution on recent dinoflagellate cysts in Izmir Bay (Eastern Aegean). Mar Pollut Bull 94:144–152

Bargagli R (2016) Moss and lichen biomonitoring of atmospheric mercury: a review. Sci Total Environ 572:216–231

Barkay T, Miller SM, Summers AO (2003) Bacterial mercury resistance from atoms to ecosystems. FEMS Microbiol Rev 27:355–384

Barros VR, Boninsegna JA, Camilloni IA et al (2015) Climate change in Argentina: trends, projections, impacts and adaptation. WIREs Clim Change 6:151–169

Battin TJ, Kaplan LA, Findlay S et al (2008) Biophysical controls on organic carbon fluxes in fluvial networks. Nat Geosci 1:95–100

Beckers F, Rinklebe J (2017) Cycling of mercury in the environment: sources, fate, and human health - A review. Crit Rev Environ Sci Technol 47:693–794

Beigt D, Villarosa G, Outes V et al (2019) Remobilized Cordón Caulle 2011 tephra deposits in North Patagonian watersheds: Resedimentation at deltaic environments and its implications. Geomorphology 341:140–152

Berenstecher P, Gangi D, Gonzalez-Arzac A et al (2017) Litter microbial and soil faunal communities stimulated in the wake of a volcanic eruption in a semi-arid woodland in Patagonia, Argentina. Funct Ecol 31:245–259

Biester H, Pérez-Rodríguez M, Gilfedder BS et al (2018) Solar irradiance and primary productivity controlled mercury accumulation in sediments of a remote lake in the Southern Hemisphere during the past 4000 years. Limnol Oceanogr 63:540–549

Bishop K, Shanley JB, Riscassi A et al (2020) Recent advances in understanding and measurement of mercury in the environment: terrestrial Hg cycling. Sci Total Environ 721:137647

Braaten HFV, Lindholm M, de Wit HA (2020) Five decades of declining methylmercury concentrations in boreal food webs suggest pivotal role for sulphate deposition. Sci Total Environ 714:136774

Branfireun BA, Cosio C, Poulain AJ et al (2020) Mercury cycling in freshwater systems - An updated conceptual model. Sci Total Environ 745:140906

Bravo AG, Cosio C (2019) Biotic formation of methylmercury: a bio–physico–chemical conundrum. Limnol Oceanogr 9999:1–18

Bravo AG, Bouchet S, Tolu J, et al (2017) Molecular composition of organic matter controlsmethylmercury formation in boreal lakes. Nat Commun 8:14255

Bubach D, Arribére MA, Ribeiro Guevara S et al (2001) Study on the feasibility of using transplanted Protousnea magellanica thalli as a bioindicator of atmospheric contamination. J Radioanal Nucl Chem 250:63–68

Bubach D, Catán SP, Arribére M et al (2012) Bioindication of volatile elements emission by the Puyehue–Cordón Caulle (North Patagonia) volcanic event in 2011. Chemosphere 88:584–590

Bubach D, Dufou L, Catán SP (2014) Evaluation of dispersal volcanic products of recent events in lichens in environmental gradient, Nahuel Huapi National Park, Argentina. Environ Monit Assess 186:4997–5007

Bushey JT, Driscoll CT, Mitchell MJ et al (2008) Mercury transport in response to storm events from a northern forest landscape. Hydrol Process 22:4813–4826

Callieri C, Modenutti B, Queimaliños C et al (2007) Production and biomass of picophytoplankton and larger autotrophs in Andean ultra- oligotrophic lakes: differences in light harvesting efficiency in deep layers. Aquat Ecol 41:511–523

Chen CY, Borsuk ME, Bugge DM et al (2014) Benthic and pelagic pathways of methylmercury bioaccumulation in estuarine food webs of the northeast United States. PLoS One 9:e89305

Chételat J, Amyot M, Garcia E (2011) Habitat-specific bioaccumulation of methylmercury in invertebrates of small mid-latitude lakes in North America. Environ Pollut 159:10–17

Chételat J, Ackerman JT, Eagles-Smith CA et al (2020) Methylmercury exposure in wildlife: a review of the ecological and physiological processes affecting contaminant concentrations and their interpretation. Sci Total Environ 711:135117

Chiaia-Hernandez AC, Ashauer R, Moest M et al (2013) Bioconcentration of organic contaminants in Daphnia resting eggs. Environ Sci Technol 47:10667–10675

Chumchal MM, Drenner RW, Fry B et al (2008) Habitat-specific differences in mercury concentration in a top predator from a shallow lake. Trans Am Fish Soc 137:195–208

Cooke CA, Martínez-Cortizas A, Bindler R et al (2020) Environmental archives of atmospheric Hg deposition – A review. Sci Total Environ 709:134800

Daga R, Ribeiro Guevara S, Sanchez ML et al (2008) Source identification of volcanic ashes by geochemical analysis of well-preserved lacustrine tephras in. Nahuel Huapi National Park. Appl Radiat Isot 66:1325–1336
Daga R, Ribeiro Guevara S, Pavlin M et al (2016) Historical records of mercury in southern latitudes over 1600 years: lake Futalaufquen. Northern Patagonia. Sci Total Environ 553:541–550
Dastoor AP, Larocque Y (2004) Global circulation of atmospheric mercury: a modeling study. Atmos Environ 38:147–161
Diaz MM, Pedrozo FL, Temporetti PF (1998) Phytoplankton of two Araucanian lakes of differing trophic status (Argentina). Hydrobiologia 369–370:45–57
Diaz MM, Pedrozo FL, Reynolds CS et al (2007) Chemical composition and the nitrogen- regulated trophic state of Patagonian lakes. Limnologica 37:17–27
Diaz SB, Paladini AA, Braile HG et al (2013) Effect on Irradiance of the eruption of the Cordón Caulle (Chile) at different altitudes in the Nahuel Huapi National Park (Patagonia, Argentina). In: First International conference on remote sensing and geoinformation of the environment (RSCy2013). Proc. SPIE 8795, 879512. https://doi.org/10.1117/12.2027517
Diéguez MC, Queimaliños CP, Ribeiro Guevara S et al (2013) Influence of dissolved organic matter character on mercury incorporation by planktonic organisms: An experimental study using oligotrophic water from Patagonian lakes. J Environ Sci 25:1980–1991
Diéguez MC, Bencardino M, García PE et al (2019) A multi-year record of atmospheric mercury species at a background mountain station in Andean Patagonia (Argentina): Temporal trends and meteorological influence. Atmos Environ 214:116819
Dranguet P, Le Faucheur S, Slaveykova VI (2017) Mercury bioavailability, transformations, and effects on freshwater biofilms. Environ Toxicol Chem 36:3194–3205
Driscoll CT, Han YJ, Chen CY et al (2007) Mercury contamination in forest and freshwater ecosystems in the northeastern United States. Bioscience 57:17–28
Driscoll CT, Mason RP, Chan HM et al (2013) Mercury as a global pollutant: sources, pathways, and effects. Environ Sci Technol 47:4967–4983
Du Preez DJ, Bencherif H, Bègue N et al (2020) Investigating the large-scale transport of a Volcanic Plume and the impact on a secondary site. Atmos 11:548
Eagles-Smith CA, Wiener JG, Eckley CS et al (2016) Mercury in western North America: a synthesis of environmental contamination, fluxes, bioaccumulation, and risk to fish and wildlife. Sci Total Environ 568:1213–1226
Eagles-Smith CA, Silbergeld EK, Basu N et al (2018) Modulators of mercury risk to wildlife and humans in the context of rapid global change. Ambio 47:170–197
Evers D (2018) The effects of Methylmercury on wildlife: a comprehensive review and approach for interpretation. In: DellaSala DA, Goldstein MI (eds) The Encyclopedia of the Anthropocene. Elsevier, Oxford, pp 181–194
Fernándes A, Falandysz J, Širič I (2020) The toxic reach of mercury and its compounds in human and animal food webs. Chemosphere 261:127765
Fernández-Gómez C, Drott A, Björn E et al (2013) Towards universal wavelength-specific photodegradation rate constants for methyl mercury in humic waters, exemplified by a Boreal lake-wetland gradient. Environ Sci Technol 47:6279–6287
Ferreyra M, Clayton S, Ezcurra C (1998) La flora altoandina de los sectores este y oeste del Parque Nacional Nahuel Huapi, Argentina. Darwiniana 36:65–79
Finley ML, Kidd KA, Curry RA et al (2016) A comparison of mercury biomagnification through lacustrine food webs supporting brook trout (*Salvelinus fontinalis*) and other salmonid fishes. Front Environ Sci 4:23
Fleck JA, Marvin-Dipasquale M, Eagles-Smith CA et al (2016) Mercury and methylmercury in aquatic sediment across western North America. Sci Total Environ 568:727–738
Gallorini A, Loizeau JL (2021) Mercury methylation in oxic aquatic macro-environments: a review. J Limnol 80. https://doi.org/10.4081/jlimnol.2021.2007
Garcia PE, Diéguez MC, Queimaliños CP (2015a) Landscape integration of North Patagonian mountain lakes: a first approach using the characterization of dissolved organic matter. Lakes Reservoirs Res Manag 20:19–32

Garcia RD, Reissig M, Queimaliños CP et al (2015b) Climate-driven terrestrial inputs in ultraoligotrophic mountain streams of Andean Patagonia revealed through chromophoric and fluorescent dissolved organic matter. Sci Total Environ 521:280–292
Garreaud R, Lopez P, Minvielle M et al (2013) Large-scale control on the Patagonian climate. J Climate 26:215–230
Garty J (2001) Biomonitoring atmospheric heavy metals with lichens: theory and application. Crit Rev Plant Sci 20:309–371
Gèntes S, Löhrer B, Legeay AF et al (2021) Drivers of variability in mercury and methylmercury bioaccumulation and biomagnification in temperate freshwater lakes. Chemosphere 267:128890
Gerea M, Pérez G, Unrein F et al (2017) CDOM and the underwater light climate in two shallow North Patagonian lakes: evaluating the effects on nano and microphytoplankton community structure. Aquat Sci. https://doi.org/10.1007/s00027-016-0493-0
Gerea M, Queimaliños C, Unrein F (2019) Grazing impact and prey selectivity of picoplanktonic cells by mixotrophic flagellates in oligotrophic lakes. Hydrobiologia. https://doi.org/10.1007/s10750-018-3610-3
Gionfriddo CM, Tate MT, Wick RR et al (2016) Microbial mercury methylation in Antarctic sea ice. Nat Microbiol 1:16127. https://doi.org/10.1038/nmicrobiol.2016.127
Graydon JA, Louis VLS, Hintelmann H et al (2008) Long-term wet and dry deposition of total and methyl mercury in the remote boreal ecoregion of Canada. Environ Sci Technol 42:8345–8351
Grégoire DS, Poulain AJ (2014) A little bit of light goes a long way: the role of phototrophs on mercury cycling. Metallomics 6:396–407
Grégoire DS, Poulain AJ (2018) Shining light on recent advances in microbial mercury cycling. Facets 3:858–879
Grigal DF (2002) Inputs and outputs of mercury from terrestrial watersheds: a review. Environ Rev 10:1–39
Gustin MS, Bank MS, Bishop K et al (2020) Mercury biogeochemical cycling: a synthesis of recent scientific advances. Sci Total Environ. https://doi.org/10.1016/j.scitotenv.2020.139619
Hanna DEL, Buck DG, Chapman LJ (2016) Effects of habitat on mercury concentrations in fish: a case study of Nile perch (*Lates niloticus*). Ecotoxicology 25:178–191
Hansen PJ, Anderson R, Stoecker DK et al (2019) Mixotrophy among freshwater and marine Protists. Reference Module in Life Sciences. https://doi.org/10.1016/b978-0-12-809633-8.20685-7
Hermanns YM, Biester H (2011) A Holocene record of mercury accumulation in a pristine lake in Southernmost South America (53°S)–climatic and environmental drivers. Biogeosci Discuss 8:6555–6588
Hermanns YM, Biester H (2013a) Anthropogenic mercury signals in lake sediments from southernmost Patagonia, Chile. Sci Total Environ 445–446:126–135
Hermanns YM, Biester H (2013b) A 17,300-year record of mercury accumulation in a pristine lake in southern Chile. J Paleo 49:547–561
Hermanns YM, Martinez Cortizas A, Arz H et al (2013) Untangling the influence of in-lake productivity and terrestrial organic matter flux on 4,250 years of mercury accumulation in Lake Hambre, Southern Chile. J Paleo 49:563–573
Higueras P, Oyarzun R, Kotnik J et al (2014) A compilation of field surveys on gaseous elemental mercury (GEM) from contrasting environmental settings in Europe, South America, South Africa and China: separating fads from facts. Environ Geochem Health. https://doi.org/10.1007/s10653-013-9591-2
Holz A, Paritsis J, Mundo IA et al (2017) Southern Annular Mode drives multicentury wildfire activity in southern South America. PNAS 114:9552–9557
Horvat M, Kotnik J (2007) Survey of gaseous elemental Hg in Patagonian transects. Internal Report Jožef Stefan Institute, Department of Environmental Sciences
Hsu-Kim H, Eckley CS, Achá D et al (2018) Challenges and opportunities for managing aquatic mercury pollution in altered landscapes. Ambio 47:141–169

Izaguirre I, Unrein F, Modenutti B et al (2014) Photosynthetic picoplankton in Argentina lakes. Adv Limnol 65:343–357

Juárez A, Arribére MA, Arcagni M et al (2016) Heavy metal and trace elements in riparian vegetation and macrophytes associated with lacustrine systems in Northern Patagonia Andean Range. Environ Sci Pollut Res 23:17995–18009

Juncos R, Milano D, Macchi PJ et al (2015) Niche segregation facilitates coexistence between native and introduced fishes in a deep Patagonian lake. Hydrobiologia 747:53–67

Kainz M, Lucotte M (2006) Mercury concentrations in lake sediments - Revisiting the predictive power of catchment morphometry and organic matter composition. Water Air Soil Pollut 170:173–189

Karimi R, Chen CY, Folt CL (2016) Comparing nearshore benthic and pelagic prey as mercury sources to lake fish: the importance of prey quality and mercury content lake fish: the importance of prey quality and mercury content. Sci Total Environ 565:211–221

Kidd KA, Bootsma HA, Hesslein RH et al (2003) Mercury concentrations in the food web of Lake Malawi, East Africa. J Great Lakes Res 29:258–266

Kocman D, Kanduč T, Ogrinc N et al (2011) Distribution and partitioning of mercury in a river catchment impacted by former mercury mining activity. Biogeochemistry 104:183–201

Kocman D, Horvat M, Pirrone N et al (2013) Contribution of contaminated sites to the global mercury budget. Environ Res 125:160–170

Kumar A, Wu S, Huang Y et al (2017) Mercury from wildfires: Global emission inventories and sensitivity to 2000–2050 global change. Atmos Environ 173:6–15

Lamborg C, Hammerschmidt C, Bowman K et al (2014) A global ocean inventory of anthropogenic mercury based on water column measurements. Nature 512:65–68

Lavoie R, Amyot M, Lapierre J-F (2019) Global meta-analysis on the relationship between mercury and dissolved organic carbon in freshwater environments. Eur J Vasc Endovasc Surg 124:1508–1523

Lehnherr I, St Louis V, Hintelmann H et al (2011) Methylation of inorganic mercury in polar marine waters. Nat Geosci 4:298–302

Lehnherr I (2014) Methylmercury biogeochemistry: a review with special reference to Arctic aquatic ecosystems. Environ Rev 22:229–243

Lyman SN, Cheng I, Gratz LE et al (2020) An updated review of atmospheric mercury. Sci Total Environ 707:135575

Marengo JA, Jones R, Alvesa LM et al (2009) Future change of temperature and precipitation extremes in South America as derived from the PRECIS regional climate modeling system. Int J Climatol 29:2241–2255

Marvin-DiPasquale M, Agee J, McGowan C et al (2000) Methyl- mercury degradation pathways: a comparison among three mercury-impacted ecosystems. Environ Sci Technol 34:4908–4916

Masiokas MH, Villalba R, Luckman BH et al (2008) 20th-century glacier recession and regional hydroclimatic changes in North-Western Patagonia. Global Planet Change 60:85–100

Masiokas M, Rivera A, Espizua LE et al (2009) Glacier fluctuations in extratropical South America during the past 1000 years. Palaeogeogr Palaeoclimatol Palaeoecol 281:242–268

Mason RP, Reinfelder JR, Morel FMM (1995) Bioaccumulation of mercury and methylmercury. Water Air Soil Pollut 80:915–921

Mason RP, Reinfelder JR, Morel FMM (1996) Uptake, toxicity, and trophic transfer of mercury in a coastal diatom. Environ Sci Technol 30:1835–1845

Mazzarino MJ, Bertiller T, Schlichter T et al (1998) Nutrient cycling in Patagonian ecosystems. Ecol Austral 8:167–181

Mermoz M, Ubeda C, Grigera D et al (2009) El parque Nacional Nahuel Huapi. Sus características ecológicas y estado de conservación. In: Parque Nacional Nahuel Huapi. APN, San Carlos de Bariloche.

Mladenov N, Sommaruga R, Morales-Baquero R et al (2011) Dust inputs and bacteria influence dissolved organic matter in clear alpine lakes. Nat Commun 2:405

Mladenov N, Williams MW, Schmidt SK et al (2012) Atmospheric deposition as a source of carbon and nutrients to an alpine catchment of the Colorado Rocky Mountains. Biogeosciences 9:3337–3355

Modenutti BE, Balseiro EG, Queimaliños CP et al (1998) Structure and dynamics of food webs in Andean lakes. Lakes Reserv Res Manag 3:179–186

Modenutti BE, Albariño RJ, Bastidas Navarro M et al (2010) Structure and dynamic of food webs in Andean North Patagonian freshwater systems: organic matter, light and nutrient relationships. Ecol Austral 20:95–114

Modenutti B, Balseiro E, Navarro MB et al (2013) Environmental changes affecting light climate in oligotrophic mountain lakes: the deep chlorophyll maxima as a sensitive variable. Aquat Sci 75:361–371

Modenutti BE, Balseiro EG, Bastidas Navarro MA et al (2016) Effects of Volcanic Pumice Inputs on microbial community composition and dissolved C/P ratios in lake waters: an experimental approach. Microb Ecol 71:18–28

Morris DP, Zagarese H, Williamson CE et al (1995) The attenuation of solar UV radiation in lakes and the role of dissolved organic carbon. Limnol Oceanogr 40:1381–1391

Mundo I, Villalba R, Veblen TT et al (2017) Fire history in southern Patagonia: human and climate influences on fire activity in *Nothofagus pumilio* forests. Ecosphere 8:e01932

Obrist D, Kirk JL, Zhang L et al (2018) A review of global environmental mercury processes in response to human and natural perturbations: changes of emissions, climate, and land use. Ambio 47:116–140

Paranjape AR, Hall BD (2017) Recent advances in the study of mercury methylation in aquatic systems. Facets 2:85–119

Pereyra FX, Bouza P (2019) Soils from the Patagonian region. In: Rubio G, Lavado RS, Pereyra FX (eds) The soils of Argentina, World Soils Book Series. Springer Nature, pp 101–121

Pérez Catán S, Arribére MA, Cohen IM (2009) Uso del ^{197}Hg como trazador de la reacción de metilación de mercurio. Análisis de la transformación biótica y abiótica de sedimentos en el lago Escondido. Rumbos Tecnológicos 1:9–22

Pérez Catán S, Arribére MA, Sánchez RS (2003) Mercury in water. In: Investigation of mercury and other heavy metals in waterbodies of Nahuel Huapi National Park, Argentine Patagonian Andean Range. Baselines determination, trophic web pathways investigation, and contamination source identification. Final Report IAEA Technical Co-operation Project ARG/7/006

Pérez Catán S, Juárez A, Bubach DF (2016) Characterization of freshwater changes in lakes of Nahuel Huapi National Park produced by the 2011 Puyehue–Cordón Caulle eruption. Environ Sci Pollut Res 23:20700–20710

Pérez Catán S, Ribeiro Guevara S, Marvin DiPasqualle M et al (2004) Determination of methyl Hg production potentials in lake Escondido sediments, Patagonia, Argentina, by using ^{197}Hg tracer. Mat Geoenvironm 51:910–914

Pérez Catán S, Ribeiro GS, Marvin-DiPasquale M et al (2007) Methodological considerations regarding the use of inorganic $^{197}Hg^{(II)}$ radiotracer to assess mercury methylation potential rates in lake sediment. Appl Radiat Isot 65:987–994

Pérez Catán S, Rodríguez Miranda M, Guimarães JRD (2011) Assessment of mercury and methylmercury in different compartments from Northwest Patagonia lakes, Argentina. In: SETAC-LA. Cumaná, Venezuela 2011

Pérez GL, Queimaliños CP, Modenutti BE (2002) Light climate and plankton in the deep chlorophyll maxima in North Patagonian Andean lakes. J Plankton Res 24:591–599

Pirrone N, Cinnirella S, Feng X et al (2010) Global mercury emissions to the atmosphere from anthropogenic and natural sources. Atmos Chem Phys 10:5951–5964

Queimaliños CP, Modenutti BE, Balseiro GE (1999) Symbiotic association of the ciliate *Ophrydium naumanni* with *Chlorella* causing a deep chlorophyll *a* maximum in an oligotrophic South Andes lake. J Plankton Res 21:167–178

Queimaliños C (2002) The role of phytoplanktonic size fractions in the microbial food webs in two north Patagonian lakes (Argentina). Arch Hydrobiol 28:1236–1240

Queimaliños C, Reissig M, Diéguez MC et al (2012) Influence of precipitation, landscape and hydrogeomorphic lake features on pelagic allochthonous indicators in two connected ultraoligotrophic lakes of North Patagonia. Sci Total Environ 427–428:219–228

Queimaliños C, Reissig M, Pérez GL et al (2019) Linking landscape heterogeneity with lake dissolved organic matter properties assessed through absorbance and fluorescence spectroscopy: spatial and seasonal patterns in temperate lakes of Southern Andes (Patagonia, Argentina). Sci Total Environ 686:223–235

Ravichandran M (2004) Interactions between mercury and dissolved organic matter - a review. Chemosphere 55:319–331

Ribeiro Guevara S, Arribere M, Calvelo S et al (1995) Elemental composition of lichens at Nahuel Huapi national park, Patagonia, Argentina. J Radioanal Nucl Chem 198:437–448

Ribeiro Guevara S, Massaferro J, Villarosa G et al (2002) Heavy metal contamination in sediments of Lake Nahuel Huapi, Nahuel Huapi National Park, Northern Patagonia, Argentina. Water Air Soil Pollut 137:21–44

Ribeiro Guevara S, Rizzo AP, Arribére MA et al (2003) Sediments. In: Investigation of mercury and other heavy metals in water bodies of Nahuel Huapi National Park, Argentine Patagonic Andean Range. Baselines determination, trophic web pathways investigation, and contamination source identification. Final Report IAEA Technical Co-operation Project ARG/7/006

Ribeiro Guevara S, Bubach D, Arribére M (2004) Mercury in lichens of Nahuel Huapi national park, Patagonia, Argentina. J Radioanal Nucl Chem 261:679–687

Ribeiro Guevara S, Rizzo A, Sánchez R et al (2005) Heavy metal inputs in Northern Patagonia lakes from short sediment cores analysis. J Radioanal Nucl Chem 265:481–493

Ribeiro Guevara S, Pérez Catán S, Marvin-DiPasquale M (2009) Benthic methylmercury production in lacustrine ecosystems of Nahuel Huapi National Park, Patagonia, Argentina. Chemosphere 77:471–477

Ribeiro Guevara S, Meili M, Rizzo A et al (2010) Sediment records of highly variable mercury inputs to mountain lakes in Patagonia during the past millennium. Atmos Chem Phys 10:3443–3453

Rizzo A, Arcagni M, Arribére MA et al (2011) Mercury in the biotic compartments of Northwest Patagonia lakes, Argentina. Chemosphere 84:70–79

Rizzo A, Arcagni M, Campbell LM et al (2014) Source and trophic transfer of mercury in plankton from an ultraoligotrophic lacustrine system (Lake Nahuel Huapi, North Patagonia). Ecotoxicology 23:1184–1194

Rizzo A, Daga R, Fajon V et al (submitted) Mercury in an ultraoligotrophic lacustrine system with volcanic sources: the relationship between soils and waters in a forested catchment

Rudolph EH (2002) Sobre la biología del camarón de río *Samastacus spinifrons* (Philippi 1882) (Decapoda, Parastacidae). Gayana 66:147–159

Schaefer JK, Jane Y, Reinfelder JR et al (2004) Role of the bacterial organomercury lyase (MerB) in controlling methylmercury accumulation in mercury-contaminated natural waters. Environ Sci Technol 38:4304–4311

Selin NE (2009) Global biogeochemical cycling of mercury: a review. Annu Rev Env Resour 34:43–63

Shanley JB, Mast MA, Campbell DH et al (2008) Comparison of total mercury and methylmercury cycling at five sites using the small watershed approach. Environ Pollut 154:143–154

Singer BS, Jicha BR, Naranjo JA et al (2008) Eruptive history, geochronology, and magmatic evolution of the Puyehue–Cordón Caulle volcanic complex, Chile. Geol Soc Am Bull 120:599–618

Soto Cárdenas C, Diéguez MC, Ribeiro Guevara S et al (2014) Incorporation of inorganic mercury (Hg^{2+}) in pelagic food webs of ultraoligotrophic and oligotrophic lakes: the role of different plankton size fractions and species assemblages. Sci Total Environ 494:65–73

Soto Cárdenas C, Gerea M, García PE et al (2017) Interplay between climate and hydrogeomorphic features and their effect on the seasonal variation of dissolved organic matter in shallow temperate lakes of the Southern Andes (Patagonia, Argentina): a field study based on optical properties. Ecohydrology 10:e1872

Soto Cárdenas C, Diéguez MC, Queimaliños CP et al (2018a) Mercury in a stream-lake network (Southern Volcanic Zone, Argentina): partitioning and interaction with dissolved organic matter. Chemosphere 197:262–270

Soto Cárdenas C, Gerea M, Queimaliños C et al (2018b) Inorganic mercury (Hg^{2+}) accumulation in autotrophic and mixotrophic planktonic protists: implications for Hg trophodynamics in ultraoligotrophic Andean Patagonian lakes. Chemosphere 199:223–231

Soto Cárdenas C, Queimaliños CP, Ribeiro Guevara S et al (2019) The microbial mercury link in oligotrophic lakes: bioaccumulation by picocyanobacteria in natural gradients of dissolved organic matter. Chemosphere 230:360–368

Sprovieri F, Pirrone N, Ebinghaus R et al (2010) A review of worldwide atmospheric mercury measurements. Atmos Chem Phys 10:8245–8265

Sprovieri F, Pirrone N, Bencardino M et al (2016) Atmospheric mercury concentrations observed at ground-based monitoring sites globally distributed in the framework of the GMOS network. Atmos Chem Phys 16:11915–11935

Stern CR (2008) Holocene tephrochronology record of large explosive eruptions in the southernmost Patagonian Andes. Bull Volcanol 70:435–454

Streets DG, Horowitz HM, Jacob DJ et al (2017) Total mercury released to the environment by human activities. Environ Sci Technol 51:5969–5977

Streets DG, Horowitz HM, Lu Z et al (2019) Global and regional trends in mercury emissions and concentrations, 2010–2015. Atmos Environ 201:417–427

Ullrich SM, Tanton TW, Abdrashitova SA (2001) Mercury in the aquatic environment: a review of factors affecting methylation. Crit Rev Environ Sci Technol 31:241–293

UNEP (2018) Global mercury assessment 2018: key findings. https://web.unep.org/globalmercurypartnership/globalmercury-assessment-2018-key-findings. Accessed 30 Sept 2021

Veblen TT, Kitzberger T (2002) Inter-hemispheric comparison of fire history: The Colorado front range, USA, and the Northern Patagonian Andes, Argentina. Plant Ecol 163:187–207

Wang X, Luo J, Yuan W et al (2020) Global warming accelerates uptake of atmospheric mercury in regions experiencing glacier retreat. PNAS 117:2049–2055

Whitney MC, Cristol DA (2018) Impacts of sublethal mercury exposure on birds: a detailed review. In: de Voogt P (ed) Reviews of environmental contamination and toxicology, reviews of environmental contamination and toxicology. Springer International Publishing, Cham, pp 113–163

Wilson R, Glasser NF, Reynolds JM (2018) Glacial lakes of the Central and Patagonian Andes. Global Planet Change 162:275–291

World Health Organization (WHO) (2017) Mercury and health. https://www.who.int/news-room/fact-sheets/detail/mercury-and-health. Accesed 25 Oct 2021

Yang L, Zhang W, Ren M et al (2020) Mercury distribution in a typical shallow lake in northern China and its reemission from sediment. Ecotoxicol Environ Saf 192:110316

Zagarese HE, Ferraro M, Queimaliños C, Diéguez MC et al (2017) Patterns of dissolved organic matter across the Patagonian landscape: a broad scale survey of Chilean and Argentine lakes. Mar Freshw Res 68:1–11

Zhang H, Yin R-S, Feng X-B, Sommar J et al (2013) Atmospheric mercury inputs in montane soils increase with elevation: evidence from mercury isotope signatures. Sci Rep 3:3322

Zhu S, Zhang Z, Žagar D (2018) Mercury transport and fate models in aquatic systems: A review and synthesis. Sci Total Environ 15:538–549